



THE UNIVERSITY *of* EDINBURGH

Edinburgh Research Explorer

## Toward Optimal Power Control and Transfer for Energy Harvesting Amplify-and-Forward Relay Networks

### Citation for published version:

Singh, K, Ku, M-L, Lin, J-C & Ratnarajah, T 2018, 'Toward Optimal Power Control and Transfer for Energy Harvesting Amplify-and-Forward Relay Networks', *IEEE Transactions on Wireless Communications*.  
<https://doi.org/10.1109/TWC.2018.2834528>

### Digital Object Identifier (DOI):

[10.1109/TWC.2018.2834528](https://doi.org/10.1109/TWC.2018.2834528)

### Link:

[Link to publication record in Edinburgh Research Explorer](#)

### Document Version:

Peer reviewed version

### Published In:

IEEE Transactions on Wireless Communications

### General rights

Copyright for the publications made accessible via the Edinburgh Research Explorer is retained by the author(s) and / or other copyright owners and it is a condition of accessing these publications that users recognise and abide by the legal requirements associated with these rights.

### Take down policy

The University of Edinburgh has made every reasonable effort to ensure that Edinburgh Research Explorer content complies with UK legislation. If you believe that the public display of this file breaches copyright please contact [openaccess@ed.ac.uk](mailto:openaccess@ed.ac.uk) providing details, and we will remove access to the work immediately and investigate your claim.



# Toward Optimal Power Control and Transfer for Energy Harvesting Amplify-and-Forward Relay Networks

Keshav Singh, *Member, IEEE*, Meng-Lin Ku, *Member, IEEE*, Jia-Chin Lin, *Senior Member, IEEE*,  
and Tharmalingam Ratnarajah, *Senior Member, IEEE*,

**Abstract**—In this paper, we study an amplify-and-forward (AF) relay network with energy harvesting (EH) source and relay nodes. Both nodes can continuously harvest energy from the environment and store it in batteries with finite capacity. Additionally, the source node is capable of transferring a portion of its energy to the relay node through a dedicated channel. The network performance depends on not only the energy arrival profiles at EH nodes but also the energy cooperation between them. We jointly design power control and transfer for maximizing the sum rate over finite time duration, subject to energy causality and battery storage constraints. By introducing auxiliary variables to confine the accumulated power expenditure, this non-convex problem is solved via a successive convex approximation (SCA) approach, and the local optimum solutions are obtained through dual decomposition. Also when channels are quasi-static and the power control values of the source (relay) node are preset to a constant, a monotonically increasing power control structure with the time is revealed for the relay (source) node with infinite battery capacity. Computer simulations are used to validate the theoretical findings and to quantify the impact of various factors such as EH intensity at nodes and relay position on the sum rate performance.

**Index Terms**—Energy harvesting, wireless power transfer, power control, amplify-and-forward, cooperative communications, optimization.

## I. INTRODUCTION

The rapid growth of the Internet-of-Things (IoT) in wireless sensor networks has received considerable attention from the research community to emphasize green wireless communications [1]–[3]. While wireless sensor nodes are often low-powered, they are typically equipped with a fixed energy source, e.g., battery, resulting in limited operation time. Frequent battery replacement is thus required for maintaining the operation of wireless sensor nodes, which is either inconvenient or expensive in hostile environment that cannot

be reached by people. Consequently, the finite capacity of batteries restrains the eventual performance of wireless sensor networks.

Cooperative communications have emerged as an effective remedy for improving the throughput, expanding the coverage and enhancing the link reliability through the use of relays. In general, the amplify-and-forward (AF) scheme has an advantage over the decode-and-forward (DF) scheme in terms of low implementation complexity [4]. Thus, we will focus on the design scenario for the AF scheme in this paper. Besides, wireless nodes participating in relay networks are often powered by finite-capacity batteries, which is a major performance bottleneck of cooperative communications [5], and this fundamental limitation motivates us to design good methodologies for recharging the batteries of wireless nodes in an AF relay network and utilizing the available energy at nodes in a more efficient way.

Recently, energy harvesting (EH) has been regarded as a promising green solution to prolong the network lifetime by scavenging energy and by supplying permanent power to wireless nodes [6]–[16]. This enables us to overcome the bottleneck of energy constraints in wireless networks [17]. In general, there are two EH methods, namely, the EH from ambient sources and the EH via wireless power transfer (WPT) [5]. The common ambient energy sources include solar, geothermal gradients of temperature, combustion, thermoelectric, hydro, piezoelectric, wind or other energy forms which are renewable, practically free of cost and environmentally friendly. Nevertheless, the fluctuation of harvested energy due to the intermittent and random nature of ambient energy sources (e.g., weather-dependent) may not guarantee wireless applications with critical quality-of-service (QoS) requirements, e.g., a minimum data rate. In result, there exists a compromise between the usage of available energy at wireless nodes and the QoS. Another potential EH solution that overcomes the random energy arrivals is to apply WPT to share the harvested energy in the batteries among nodes [18]–[23]. In practice, WPT can be carried out through scavenging energy from the radio frequency (RF) signals sent by a dedicated transmitter.

In this paper, we revisit the design of AF relay networks with EH and power transfer capability. The uncertainty of energy sources and the variation of channel fading create several challenges in designing such networks. First, the energy harvested by the source and the relay nodes is independent in terms of arrivals and amounts during the course of data

Manuscript received October 20, 2017; revised January 29, 2018 and April 23, 2018; accepted May 1, 2018. The associate editor coordinating the review of this manuscript and approving it for publication was Dr. Bruno Clerckx.

This work was supported by the Ministry of Science and Technology of Taiwan under Grant MOST 106-2221-E-008-014 and the U.K. Engineering and Physical Sciences Research Council (EPSRC) under Grant EP/N014073/1.

Keshav Singh, Meng-Lin Ku, and Jia-Chin Lin are with the Department of Communication Engineering, National Central University, Taiwan. (e-mail: {mlku, jiachin}@ce.ncu.edu.tw).

Keshav Singh and Tharmalingam Ratnarajah are with School of Engineering, University of Edinburgh, Edinburgh, UK. (e-mail: {k.singh, t.ratnarajah}@ed.ac.uk).

The corresponding author of this paper is Meng-Lin Ku.

transmission. Second, the random nature of ambient energy sources necessitates a dynamic power control mechanism to efficiently reflect upon energy utilization processes in the battery. Third, the channel path loss phenomenon causes an energy loss problem, resulting in a tradeoff between the information and the power transfer from the source to the relay nodes. Thus, how to efficiently utilize the harvested energy to maximize the sum rate of an AF relay network is still an open issue.

Several power control schemes have been investigated for EH wireless communications [6]–[15]. A resource allocation policy was proposed in [6] to maximize a network utility under EH constraints. Based on the non-causal knowledge of energy arrivals over time, a power control policy was derived in [8] for an energy transmitter to minimize the transmission completion time for a given amount of data with an unlimited energy buffer. The authors in [9] extended [8] to the scenario of a transmitter with a finite battery size for short-term throughput maximization, while the throughput maximization problems for the applications in fading channels were studied in [10] and [11], wherein a water-filling solution was proven to be the optimal energy allocation. Besides, EH was applied in cooperative networks to enhance the network throughput. In [13], a two-hop EH DF relay network was investigated with one-way power transfer from a source node to a relay node, and a two-dimensional directional water-filling algorithm was proposed for maximizing the data throughput. However, the throughput maximization problem in [13] was formulated with energy and data causality constraints for DF relay networks with the assumption of infinite battery capacity at the source and the relay nodes. Moreover, the proposed policies in [13] cannot be directly applied for AF relay networks due to the non-convexity of the sum rate formula in the AF protocol, which is resulted from a noise enhancement problem when relaying signals from the source to the destination. The power control schemes for DF relay networks were studied in [14], subject to EH constraints. Paper [15] extended [14] to a scenario in which multiple source-and-destination pairs communicate via an EH DF relay. In [16], a cooperative network was studied, and EH nodes can serve as AF relays if they own sufficient energy for helping transmissions.

Apart from conventional EH techniques, the WPT has also been studied in the literature [18]–[22]. The architecture and deployment issues for the WPT were studied in [18], where an uplink cellular network overlays with randomly deployed power stations for wirelessly powering mobile devices by microwave radiation. In [19], time-sharing or power-splitting approaches were proposed for simultaneous wireless information and power transfer (SWIPT) systems. A performance tradeoff between information and power transfer was later analyzed in [20] for point-to-point communications in flat fading channels, while the authors in [21] extended the work of [20] to frequency selective fading channels. In [22] and [23], a rate-energy region was characterized to demonstrate the performance tradeoff in essence. In [24], transmit power allocation and energy cooperation policies that jointly maximize the sum rate of a full-duplex DF relay network were investigated. However, the sum rate maximization problem in

[24] was formulated under energy causality constraints with the strong assumption of infinite battery capacity at source and relay nodes. Additionally, the design framework in [24] cannot be directly applied for AF relay networks, since the sum rate formula for AF relay networks is non-convex. Minasian *et al.* [25] proposed an optimal power allocation policy to maximize the throughput of an EH AF relay network under a high signal-to-noise ratio (SNR) approximation and without energy cooperation between source and relay nodes. By using power splitting or time switching protocols, SWIPT systems were studied in [26] for minimizing the outage probability of two-way DF relay networks. The works of [27]–[30] extended the study in multi-relay networks. Based on different channel state information requirements and implementation complexities, the authors in [27] proposed several relay selection policies for wireless-powered DF relay networks, while a relay selection scheme was investigated in [28] under a timing structure for enabling EH, relay selection, and AF information relaying. The authors in [29] extended the designs of [27] and [28] to multi-relay selection. In [30], a distributed power splitting scheme was studied for relay interference channels by using the game theory.

The majority of the aforementioned works [13], [18]–[30] focused on either EH or power transfer with AF or DF protocols under some assumptions, e.g., high SNRs, infinite battery capacity, but to the best of our knowledge, the sum rate maximization problem with joint consideration of EH and power transfer has not been investigated under AF protocols with both energy causality and battery storage constraints. In this paper, we consider a joint design of power control and transfer for a three-node AF relay network with energy transmitters (source/relay) and unidirectional power transfer from the source to the relay nodes. The source's ambient harvested energy could be conveyed to the relay by WPT via a dedicated energy control channel which occupies a certain small bandwidth and has a sufficiently large frequency separation from the data transmission channel. For example, the EH source node can utilize distinct frequencies (e.g., 868MHz and 2.4GHz unlicensed bands) for delivering data and the ambient harvested energy to the EH relay node simultaneously [31]–[35]. Although the wireless power can be transmitted over multiple frequencies [36]–[38], this paper focuses on the scenario where power is delivered through a single frequency tone. In our work, the EH nodes are capable of scavenging ambient energy from the environment, e.g., solar, and storing the harvested energy in finite-capacity batteries over multiple time slots. On the contrary, the SWIPT systems in the literature, e.g., [19], are mainly related to wireless information and power transfer without considering the ambient EH. Further, these works do not consider the storage of the harvested energy in a battery with finite capacity over multiple time slots. At this point we would like to note that the studied system in this paper may share similarities to traditional AF relay networks, in terms of the system concept, service requirements, design guidelines, and optimization skills. However, applying EH and power transfer technology and maximizing the sum rate bring in itself new intrinsic sets of challenges. In particular, the main distinctions and contributions are encapsulated as below.

- In contrast to [13], [18]–[30], we focus on joint optimization of power control and transfer for EH AF relay networks by formulating a sum rate maximization problem under energy causality and battery storage constraints. The problem is challenging to solve due to its non-convexity.
- By utilizing the lower bound approximation in [39], the non-convex problem is transformed into a tractable convex problem under the given values of auxiliary variables.
- Based on the dual decomposition in [40], an iterative power control and transfer algorithm is proposed in the inner loop by solving a sequence of sub-problems. A two-step method is then proposed in the outer loop to determine the values of auxiliary variables. To achieve the optimal solution, theoretical results show that at the end of transmissions, the source node has to exhaust the harvested energy either for data transmission or WPT. Similarly, the relay node has to exhaust all of its harvested energy either from the environment or the source node for relaying.
- We analyze the impact of infinite battery size on the optimal transmission policy and also study the problem with infinite battery capacity at the EH source node or the EH relay node when the relay's or the source's power control are preset to a constant value. The assumption of the infinite battery size is generally true for low-powered wireless nodes with relatively large capacitors. It reveals that when the capacity of the source's (relay's) battery is infinite and channels are quasi-static over time, the source's (relay's) power control value is non-decreasing with the time index, if relay's (source's) transmit power is constant.
- As compared with the scenario without applying the power transfer or the direct transmission of the EH source node without relaying, the proposed design can greatly improve the sum rate performance.

The remainder of this paper is organized as follows. We present the system model and problem formulation in Section II. The procedure of transforming the non-convex joint design problem into a convex one is described in Section III, along with the exploration of the properties of the optimal power control and transfer solution<sup>1</sup>. In addition, an iterative power control and transfer algorithm is proposed via dual decomposition. The optimal power control values with infinite battery capacity at either the source node or the relay node are analyzed in Section IV. A weighted sum mean-squared-error (sum-MSE) minimization problem is illustrated in Section V for comparison. Numerical results are given in Section VI. Finally, conclusions are drawn in Section VII.

## II. SYSTEM MODEL AND PROBLEM FORMULATION

### A. System Model

Fig. 1 shows an EH AF relay network, consisting of one source node ( $S$ ), one relay node ( $R$ ), and one destination node ( $D$ ). It is assumed that each node in the network is

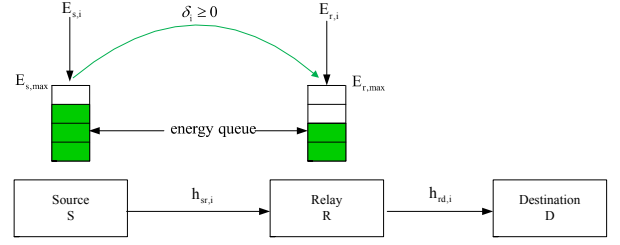


Fig. 1: An EH AF relay network.

equipped with a single antenna. For simplicity, we further assume that there is no direct link available between the source and the destination nodes due to a poor channel condition between them. Both the source and relay nodes are capable of harvesting energy from ambient energy sources (e.g., solar) and storing the harvested energy in finite energy queues, i.e., batteries, for the forthcoming data transmissions. A time slotted model with a slot length of  $T$  is considered in this paper, and without loss of generality, the time duration for each slot is assumed to be one. The energy queues at the source and the relay nodes can store at most  $E_{s,max}$  and  $E_{r,max}$  units of energy, respectively, and the status of the energy queues at both nodes is updated in the end of each time slot. In addition, the wireless channels between any two nodes are frequency flat fading and quasi-static within each time slot. A common two-phase transmission protocol is adopted for each time slot in the AF relay network for transmitting data from the source node to the destination node via the intermediate relay.

In the first phase, the source node sends data signals toward the relay node, while in the second phase, the relay node forwards the amplified signals to the destination node; meanwhile, the source node keeps silent. Hence, the received signal,  $y_{r,i}$ , at the relay in the first phase can be expressed as

$$y_{r,i} = \sqrt{P_{s,i}} h_{sr,i} x_{s,i} + n_{r,i}, \quad i = 1, \dots, T, \quad (1)$$

where the subscript index  $i$  indicates the  $i^{th}$  time slot,  $P_{s,i}$  is the source's transmit power,  $h_{sr,i}$  represents the channel coefficient from the source node to the relay node,  $x_{s,i}$  is the source's transmitted data signal with unit power, i.e.  $\mathbb{E}[|x_{s,i}|^2] = 1$ , and  $n_{r,i}$  is additive white Gaussian noise (AWGN) at the relay with zero mean and variance  $\sigma_r^2$ . Define the channel power values  $g_{sr,i} = |h_{sr,i}|^2$  and  $g_{rd,i} = |h_{rd,i}|^2$ , for  $i = 1, \dots, T$ . In the second phase, the received signal,  $y_{d,i}$ , at the destination node is stated as

$$\begin{aligned} y_{d,i} &= h_{rd,i} x_{r,i} + n_{d,i} \\ &= \underbrace{\frac{\sqrt{P_{s,i} P_{r,i}}}{\sqrt{P_{s,i} g_{sr,i} + \sigma_r^2}} h_{rd,i} h_{sr,i} x_{s,i}}_{\text{desired signal}} \\ &\quad + \underbrace{\frac{\sqrt{P_{r,i}}}{\sqrt{P_{s,i} g_{sr,i} + \sigma_r^2}} h_{rd,i} n_{r,i} + n_{d,i}}_{\text{compound noise}}, \quad i = 1, \dots, T, \quad (2) \end{aligned}$$

where  $P_{r,i}$ ,  $h_{rd,i}$ ,  $n_{d,i}$  and  $\sigma_d^2$  are defined similar to  $P_{s,i}$ ,  $h_{sr,i}$ ,  $n_{r,i}$  and  $\sigma_r^2$ , respectively, but they are now associated with the channel link from the relay to the destination nodes, and  $x_{r,i} =$

<sup>1</sup>The optimal solution is referred as local optimum solution.

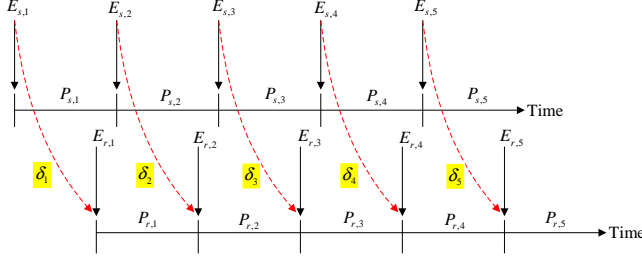


Fig. 2: A slotted power control and EH model.

$\frac{\sqrt{P_{r,i}}}{\sqrt{P_{s,i}g_{sr,i} + \sigma_r^2}} y_{r,i}$  is the transmitted signal of the relay node after signal amplification. According to the capacity formula in [41], the sum rate,  $f_R(\mathbf{P}_s, \mathbf{P}_r)$ , during the  $T$  time slots is given by

$$f_R(\mathbf{P}_s, \mathbf{P}_r) = \frac{1}{2} \sum_{i=1}^T \log_2(1 + \Gamma_i), \quad (3)$$

where  $\mathbf{P}_s = (P_{s,1}, P_{s,2}, \dots, P_{s,T})$ ,  $\mathbf{P}_r = (P_{r,1}, P_{r,2}, \dots, P_{r,T})$ , and the SNR at the destination node is given by

$$\Gamma_i = \frac{P_{s,i} P_{r,i} g_{rd,i} g_{sr,i}}{P_{r,i} g_{rd,i} \sigma_r^2 + \sigma_d^2 (P_{s,i} g_{sr,i} + \sigma_r^2)}, \quad i = 1, \dots, T. \quad (4)$$

### B. Sum Rate Maximization for Joint Power Control and Transfer

Here we formulate the sum rate maximization problem for the joint design of power control and transfer in the AF relay network. It is assumed that the amounts of the harvested energy for the source and the relay nodes at the  $i^{th}$  time slot are given as  $E_{s,i}$  and  $E_{r,i}$ , respectively, and the energy profiles are non-causally known before data transmission. Fig. 2 illustrates a slotted power control and EH model, and for the convenience of illustration, the EH profile of the relay node is indexed with one slot delay with respect to that of the source node so that the time slot index in the formulated optimization problem can be aligned. Furthermore, the source node is able to utilize an additional dedicated energy control channel for simultaneously transferring  $\delta_i \geq 0$  amount of energy to the relay node at the  $i^{th}$  time slot. By doing so, the source node can possibly share a portion of its harvested energy, if abundant enough, with the relay node to prolong the network lifetime of cooperative communications. Consequently, the energy available at the source and relay nodes at the time slot  $i$  is controlled by the following factors: (i) the harvested energy,  $E_{s,i}$  and  $E_{r,i}$ ; (ii) the energy transferred from the source node to the relay node  $\delta_i$ ; (iii) the energy received by the relay node from the source node, and (iv) the energy consumed for data transmission  $P_{s,i}$  and  $P_{r,i}$ .

Due to the random nature of the harvested energy and the finite battery capacity, the power control and transfer are primarily subject to two kinds of energy constraints: (i) energy causality constraints and (ii) battery storage constraints. Specifically, for the causality constraints, it means that the harvested energy cannot be utilized until it arrives. That is, the energy causality constraints for the power control and transfer

at the source and the relay nodes in time are respectively given by

$$(C.1) \quad \sum_{i=1}^k P_{s,i} \leq \sum_{i=1}^k (E_{s,i} - \delta_i), \quad k = 1, \dots, T; \quad (5)$$

$$(C.2) \quad \sum_{i=1}^k P_{r,i} \leq \sum_{i=1}^k (E_{r,i} + \alpha \bar{g}_{sr,i} \delta_i), \quad k = 1, \dots, T, \quad (6)$$

where  $\alpha$  is the power harvesting and conversion efficiency, ranging between 0 and 1, and  $\bar{g}_{sr,i}$  indicates the channel power gain of the dedicated energy control channel at the  $i^{th}$  time slot. Besides, the battery storage constraints stipulate that the amount of energy stored in the battery never exceeds the maximum battery capacity at the source and the relay nodes:

$$(C.3) \quad \sum_{i=1}^{k+1} (E_{s,i} - \delta_i) - \sum_{i=1}^k P_{s,i} \leq E_{s,max}, \quad k = 1, \dots, T-1; \quad (7)$$

$$(C.4) \quad \sum_{i=1}^{k+1} (E_{r,i} + \alpha \bar{g}_{sr,i} \delta_i) - \sum_{i=1}^k P_{r,i} \leq E_{r,max}, \quad k = 1, \dots, T-1, \quad (8)$$

where  $E_{s,max}$  and  $E_{r,max}$  are the battery capacity of the source and the relay nodes, respectively.

From (3)–(8), the joint design problem of the power control and transfer for the sum rate maximization is then formulated as

$$(\mathbf{P1}) : \max_{\mathbf{P}_s \geq 0, \mathbf{P}_r \geq 0, \delta \geq 0} f_R(\mathbf{P}_s, \mathbf{P}_r) \quad \text{s.t.} \quad (C.1), (C.2), (C.3) \ \& \ (C.4), \quad (9)$$

where  $\delta = (\delta_1, \delta_2, \dots, \delta_T)$ .

## III. OPTIMAL POWER CONTROL AND TRANSFER

### A. Transformation into Convex Optimization Problem

Notice that the involved constraints in (9) are all convex, whereas the objective function  $f_R(\mathbf{P}_s, \mathbf{P}_r)$  is non-concave. Hence, the problem (P1) is challenging and cannot be solved in its current form by utilizing standard convex optimization techniques [42]. To make the problem tractable, we resort to change of variables and an SCA approach to convert the non-convex optimization problem into a convex one. By letting  $\bar{P}_{s,i} = \log P_{s,i}$  and  $\bar{P}_{r,i} = \log P_{r,i}$ , the problem (P1) can be equivalently transformed as

$$(\mathbf{P2}) : \max_{\bar{\mathbf{P}}_s, \bar{\mathbf{P}}_r, \delta \geq 0} \bar{f}_R(\bar{\mathbf{P}}_s, \bar{\mathbf{P}}_r) \quad \text{s.t.} \quad (C.1) \quad \sum_{i=1}^k e^{\bar{P}_{s,i}} \leq \sum_{i=1}^k (E_{s,i} - \delta_i), \quad k = 1, \dots, T; \quad (C.2) \quad \sum_{i=1}^k e^{\bar{P}_{r,i}} \leq \sum_{i=1}^k (E_{r,i} + \alpha \bar{g}_{sr,i} \delta_i), \quad k = 1, \dots, T; \quad (C.3) \quad \sum_{i=1}^{k+1} (E_{s,i} - \delta_i) - \sum_{i=1}^k e^{\bar{P}_{s,i}} \leq E_{s,max}, \quad k = 1, \dots, T-1; \quad (C.4) \quad \sum_{i=1}^{k+1} (E_{r,i} + \alpha \bar{g}_{sr,i} \delta_i) - \sum_{i=1}^k e^{\bar{P}_{r,i}} \leq E_{r,max}, \quad k = 1, \dots, T-1;$$

where  $\bar{\mathbf{P}}_s = (\bar{P}_{s,1}, \bar{P}_{s,2}, \dots, \bar{P}_{s,T})$ ,  $\bar{\mathbf{P}}_r = (\bar{P}_{r,1}, \bar{P}_{r,2}, \dots, \bar{P}_{r,T})$ ,  $\bar{f}_R(\bar{\mathbf{P}}_s, \bar{\mathbf{P}}_r) = \frac{1}{2} \sum_{i=1}^T \log_2(1 + \bar{\Gamma}_i)$ , and

$$\bar{\Gamma}_i = \frac{e^{\bar{P}_{s,i} + \bar{P}_{r,i}} g_{rd,i} g_{sr,i}}{e^{\bar{P}_{r,i}} g_{rd,i} \sigma_r^2 + \sigma_d^2 (e^{\bar{P}_{s,i}} g_{sr,i} + \sigma_r^2)}. \quad (11)$$

A closer look at (10) reveals that the constraints (C.1) and (C.2) remain convex after the change of variables; however, the constraints (C.3) and (C.4) are non-convex in terms of  $\bar{P}_{s,i}$  and  $\bar{P}_{r,i}$ . By introducing auxiliary variables  $\Omega_{s,k} = \sum_{i=1}^k e^{\bar{P}_{s,i}}$  and  $\Omega_{r,k} = \sum_{i=1}^k e^{\bar{P}_{r,i}}$  and relaxing the equality constraints, it yields the following optimization problem:

$$\begin{aligned} (\mathbf{P3}) : \quad & \max_{\bar{\mathbf{P}}_s, \bar{\mathbf{P}}_r, \delta \geq 0, \Omega_s, \Omega_r} \bar{f}_R(\bar{\mathbf{P}}_s, \bar{\mathbf{P}}_r) \\ \text{s.t.} \quad & (C.1) \quad \sum_{i=1}^k e^{\bar{P}_{s,i}} \leq \sum_{i=1}^k (E_{s,i} - \delta_i), \quad k = 1, \dots, T; \\ & (C.2) \quad \sum_{i=1}^k e^{\bar{P}_{r,i}} \leq \sum_{i=1}^k (E_{r,i} + \alpha \bar{g}_{sr,i} \delta_i), \\ & \quad \quad \quad k = 1, \dots, T; \\ & (C.3) \quad \sum_{i=1}^{k+1} (E_{s,i} - \delta_i) - \Omega_{s,k} \leq E_{s,max}, \\ & \quad \quad \quad k = 1, \dots, T-1; \\ & (C.4) \quad \sum_{i=1}^{k+1} (E_{r,i} + \alpha \bar{g}_{sr,i} \delta_i) - \Omega_{r,k} \leq E_{r,max}, \\ & \quad \quad \quad k = 1, \dots, T-1; \\ & (C.5) \quad \sum_{i=1}^k e^{\bar{P}_{s,i}} \leq \Omega_{s,k}, \quad k = 1, \dots, T-1; \\ & (C.6) \quad \sum_{i=1}^k e^{\bar{P}_{r,i}} \leq \Omega_{r,k}, \quad k = 1, \dots, T-1, \end{aligned} \quad (12)$$

where  $\Omega_s = (\Omega_{s,1}, \Omega_{s,2}, \dots, \Omega_{s,T-1})$  and  $\Omega_r = (\Omega_{r,1}, \Omega_{r,2}, \dots, \Omega_{r,T-1})$  can be regarded as accumulated power expenditure profiles. Now the constraints in the problem (P3) are all convex if the values of the auxiliary variables are given. Since the transformed objective function is still non-concave, we further adopt an SCA approach to convert the problem (P3) into a tractable one by maximizing a lower bound of the achievable sum rate in the following:

$$\begin{aligned} (\mathbf{P4}) : \quad & \max_{\bar{\mathbf{P}}_s, \bar{\mathbf{P}}_r, \delta \geq 0, \Omega_s, \Omega_r} \bar{f}_{LB}(\bar{\mathbf{P}}_s, \bar{\mathbf{P}}_r) \\ \text{s.t.} \quad & (C.1) - (C.6) \text{ in (12)}, \end{aligned} \quad (13)$$

where  $\bar{f}_{LB}(\bar{\mathbf{P}}_s, \bar{\mathbf{P}}_r)$  is given as

$$\bar{f}_{LB}(\bar{\mathbf{P}}_s, \bar{\mathbf{P}}_r) = \frac{1}{2} \sum_{i=1}^T \left[ \rho_i \log_2(\bar{\Gamma}_i) + \beta_i \right] \leq \bar{f}_R(\bar{\mathbf{P}}_s, \bar{\mathbf{P}}_r), \quad (14)$$

and the relationship of the lower bound is always valid if the coefficients  $\rho_i$  and  $\beta_i$  are chosen as [39]

$$\rho_i = \gamma_i / (1 + \gamma_i); \quad (15)$$

$$\beta_i = \log_2(1 + \gamma_i) - \rho_i \log_2(\gamma_i), \quad (16)$$

for any  $\gamma_i > 0$ . In particular, the lower bound (14) becomes tight with equality at  $\gamma_i = \bar{\Gamma}_i$  when the coefficients  $\rho_i$  and  $\beta_i$  are selected as specified above.

*Lemma 1:* For given coefficients  $\rho_i$  and  $\beta_i$ ,  $\bar{f}_{LB}(\bar{\mathbf{P}}_s, \bar{\mathbf{P}}_r)$  is a concave function of  $\bar{\mathbf{P}}_s$  and  $\bar{\mathbf{P}}_r$ .

*Proof:* By substituting the definition of  $\bar{\Gamma}_i$  in (11) into  $\bar{f}_{LB}(\bar{\mathbf{P}}_s, \bar{\mathbf{P}}_r)$  in (14), we get

$$\begin{aligned} \bar{f}_{LB}(\bar{\mathbf{P}}_s, \bar{\mathbf{P}}_r) &= \frac{1}{2} \sum_{i=1}^T \left[ \rho_i \log_2(\bar{\Gamma}_i) + \beta_i \right] \\ &= \frac{1}{2} \sum_{i=1}^T \left[ \frac{\rho_i}{\log_2} \left\{ \bar{P}_{s,i} + \bar{P}_{r,i} + \log(g_{rd,i} g_{sr,i}) \right. \right. \\ &\quad \left. \left. - \log \left( e^{\bar{P}_{r,i}} g_{rd,i} \sigma_r^2 + \sigma_d^2 (e^{\bar{P}_{s,i}} g_{sr,i} + \sigma_r^2) \right) \right\} + \beta_i \right]. \end{aligned} \quad (17)$$

The function  $\bar{f}_{LB}(\bar{\mathbf{P}}_s, \bar{\mathbf{P}}_r)$  is concave, since it consists of the sum of affine terms and concave terms within the square brackets. (Note that the log-sum-exp function is convex [42].) ■

From Lemma 1, it is known that the problem (P4) is convex if the coefficients  $\rho_i$  and  $\beta_i$  and the auxiliary variables  $\Omega_{s,k}$  and  $\Omega_{r,k}$  are given.

Next, we provide a theorem regarding the update of the coefficients  $\rho_i$  and  $\beta_i$ , as follows:

*Theorem 1:* By fixing  $\Omega_s$  and  $\Omega_r$ , let  $(\bar{\mathbf{P}}_s^{(t)}, \bar{\mathbf{P}}_r^{(t)})$  be the optimal solution of the problem (P4) with respect to  $\rho_i^{(t)}$  and  $\beta_i^{(t)}$  at the  $t^{th}$  iteration. If the coefficients  $\rho_i$  and  $\beta_i$  are updated as

$$\begin{aligned} \rho_i^{(t+1)} &= \bar{\Gamma}_i^{(t)} / (1 + \bar{\Gamma}_i^{(t)}); \\ \beta_i^{(t+1)} &= \log_2(1 + \bar{\Gamma}_i^{(t)}) - \rho_i^{(t)} \log_2(\bar{\Gamma}_i^{(t)}), \end{aligned} \quad (18)$$

the optimal value of  $\bar{f}_{LB}(\bar{\mathbf{P}}_s^{(t)}, \bar{\mathbf{P}}_r^{(t)}, \rho_i^{(t)}, \beta_i^{(t)})$  for the problem (P4) increases monotonically with respect to  $t$ , where  $\bar{\Gamma}_i^{(t)}$  is obtained by replacing  $(\bar{\mathbf{P}}_s^{(t)}, \bar{\mathbf{P}}_r^{(t)})$  into (11).

*Proof:* Since  $(\bar{\mathbf{P}}_s^{(t)}, \bar{\mathbf{P}}_r^{(t)})$  is the optimal solution of the problem (P4) in (13) with respect to the coefficients  $\rho_i^{(t)}$  and  $\beta_i^{(t)}$  at the  $t^{th}$  iteration. If  $\rho_i^{(t+1)}$  and  $\beta_i^{(t+1)}$  are updated according to (18), we can get

$$\begin{aligned} \bar{f}_{LB}(\bar{\mathbf{P}}_s^{(t)}, \bar{\mathbf{P}}_r^{(t)}, \rho_i^{(t)}, \beta_i^{(t)}) &\leq \bar{f}_R(\bar{\mathbf{P}}_s^{(t)}, \bar{\mathbf{P}}_r^{(t)}) \\ &= \bar{f}_{LB}(\bar{\mathbf{P}}_s^{(t)}, \bar{\mathbf{P}}_r^{(t)}, \rho_i^{(t+1)}, \beta_i^{(t+1)}); \\ &\leq \bar{f}_{LB}(\bar{\mathbf{P}}_s^{(t+1)}, \bar{\mathbf{P}}_r^{(t+1)}, \rho_i^{(t+1)}, \beta_i^{(t+1)}), \end{aligned} \quad (19)$$

where the first inequality and the second equality follow from the definition in (14)–(16), while the third inequality is because of the optimization problem (P4) in (13). Consequently, the lower bound performance increases monotonically with the update of the coefficients  $\rho_i$  and  $\beta_i$ . ■

### B. Properties of the Optimal Power Control and Transfer Solution

Before we solve the joint design problem (P2) via the convex problem (P4), some essential properties of the optimal power control and transfer solution of the problem (P4) are provided in this subsection.

**Lemma 2:** The sum rate function  $\bar{f}_{LB}(\bar{\mathbf{P}}_s, \bar{\mathbf{P}}_r)$  is a monotonically increasing function of  $\bar{\mathbf{P}}_s$  and  $\bar{\mathbf{P}}_r$ .

*Proof:* From (11), we can rewrite  $\bar{\Gamma}_i$  as

$$\bar{\Gamma}_i = \left( \frac{\sigma_r^2}{e^{\bar{P}_{s,i}} g_{sr,i}} + \frac{\sigma_d^2}{e^{\bar{P}_{r,i}} g_{rd,i}} + \frac{\sigma_d^2 \sigma_r^2}{e^{\bar{P}_{s,i} + \bar{P}_{r,i}} g_{rd,i} g_{sr,i}} \right)^{-1}. \quad (20)$$

It is seen that  $\bar{\Gamma}_i$  is an increasing function of  $\bar{P}_{s,i}$  and  $\bar{P}_{r,i}$ , and thus, the sum rate function  $\bar{f}_{LB}(\bar{\mathbf{P}}_s, \bar{\mathbf{P}}_r)$  is an increasing function of  $\bar{\mathbf{P}}_s$  and  $\bar{\mathbf{P}}_r$ . ■

**Theorem 2:** The optimal power control and transfer profiles  $P_{s,i}^* = e^{\bar{P}_{s,i}^*}$ ,  $P_{r,i}^* = e^{\bar{P}_{r,i}^*}$ , and  $\delta_i^*$  of the problem (P4) must satisfy  $\sum_{i=1}^T P_{s,i}^* = \sum_{i=1}^T (E_{s,i} - \delta_i^*)$ .

*Proof:* We prove this theorem by contradiction. Assume that  $\sum_{i=1}^T P_{s,i}^* < \sum_{i=1}^T (E_{s,i} - \delta_i^*)$  is true for the optimal solution  $(P_{s,i}^*, P_{r,i}^*, \delta_i^*, \Omega_{s,k}^*, \Omega_{r,k}^*)$ . Then we can increase  $P_{s,T}^*$  to achieve a higher sum rate of  $\bar{f}_{LB}(\bar{\mathbf{P}}_s, \bar{\mathbf{P}}_r)$  by applying Lemma 2 without conflicting any other constraints in (13). Hence, it contradicts the optimality of  $(P_{s,i}^*, P_{r,i}^*, \delta_i^*, \Omega_{s,k}^*, \Omega_{r,k}^*)$ . ■

**Theorem 3:** The optimal power control and transfer profiles  $P_{s,i}^* = e^{\bar{P}_{s,i}^*}$ ,  $P_{r,i}^* = e^{\bar{P}_{r,i}^*}$ , and  $\delta_i^*$  of the problem (P4) must satisfy  $\sum_{i=1}^T P_{r,i}^* = \sum_{i=1}^T (E_{r,i} + \alpha \bar{g}_{sr,i} \delta_i^*)$ .

*Proof:* This theorem can be proved by contradiction as follows. Suppose this constraint is satisfied with strict inequality, i.e.,  $\sum_{i=1}^T P_{r,i}^* < \sum_{i=1}^T (E_{r,i} + \alpha \bar{g}_{sr,i} \delta_i^*)$  for the optimal solution  $(P_{s,i}^*, P_{r,i}^*, \delta_i^*, \Omega_{s,k}^*, \Omega_{r,k}^*)$ . Then we can decrease  $\delta_T^*$  and increase  $P_{s,T}^*$  and  $\Omega_{s,T-1}^*$  to achieve a higher sum rate, while satisfying any other constraints in (13). This contradicts the optimality of  $(P_{s,i}^*, P_{r,i}^*, \delta_i^*, \Omega_{s,k}^*, \Omega_{r,k}^*)$ . ■

Theorem 2 and Theorem 3 reveal some interesting findings about the optimal solutions of the power control and transfer. We can observe from Theorem 2 that the source node has to exhaust the entire harvested energy at the end of transmissions either for data transmission or in the form of WPT for attaining the optimal sum rate performance. Theorem 3 indicates that at the end of transmissions, the relay node has to exhaust all of its harvested energy from the source node or the ambient environment for forwarding the signals to the destination node.

### C. Optimal Power Control and Transfer Algorithm Under Fixed Values of Auxiliary Variables

By fixing the values of the auxiliary variables  $\Omega_{s,k}$  and  $\Omega_{r,k}$  and the coefficients  $\rho_i$  and  $\beta_i$ , the problem (P4) is a convex optimization problem, which can be efficiently solved using standard convex optimization tools, e.g., CVX [42].

To get more insight into the optimal solution, an iterative algorithm is proposed for solving the problem by applying a dual decomposition approach. Since the primal problem (P4) in (13) is convex and satisfies the Slater's condition, the optimal solution can be obtained by considering its dual problem as follows [42]:

$$\min_{\lambda, \mu, \eta, \nu, \vartheta, \kappa \geq 0} \max_{\bar{\mathbf{P}}_s, \bar{\mathbf{P}}_r, \delta \geq 0} \mathcal{L}(\bar{\mathbf{P}}_s, \bar{\mathbf{P}}_r, \delta, \lambda, \mu, \eta, \nu, \vartheta, \kappa). \quad (21)$$

Note that the Lagrangian function  $\mathcal{L}(\bar{\mathbf{P}}_s, \bar{\mathbf{P}}_r, \delta, \lambda, \mu, \eta, \nu, \vartheta, \kappa)$  for the optimization problem in (13) can be expressed as in (22) shown on the top of next page, where  $\lambda = (\lambda_1, \dots, \lambda_T)$  and  $\mu = (\mu_1, \dots, \mu_T)$  are the Lagrangian multiplier vectors associated with the energy causality constraints (C.1) and (C.2), respectively. The Lagrangian multiplier vectors  $\eta = (\eta_1, \dots, \eta_{T-1})$  and  $\nu = (\nu_1, \dots, \nu_{T-1})$  are corresponding to the battery storage constraints (C.3) and (C.4), respectively, while  $\vartheta = (\vartheta_1, \dots, \vartheta_{T-1})$  and  $\kappa = (\kappa_1, \dots, \kappa_{T-1})$  are the Lagrangian multiplier vectors for the auxiliary constraints (C.5) and (C.6), respectively. Notice that the values of these Lagrangian multipliers are non-negative.

The problem is then decomposed and solved via two iterative steps: (i) the first step is related to a subproblem for finding the solutions of the power control and transfer, and (ii) the second step involves a master dual problem for updating the Lagrangian multipliers.

1) *Subproblem Solution (Update of  $\bar{\mathbf{P}}_s$ ,  $\bar{\mathbf{P}}_r$  and  $\delta$ ):* For a fixed set of Lagrangian multipliers, the inner maximization problem is given as

$$\max_{\bar{\mathbf{P}}_s, \bar{\mathbf{P}}_r, \delta \geq 0} \mathcal{L}(\bar{\mathbf{P}}_s, \bar{\mathbf{P}}_r, \delta, \lambda, \mu, \eta, \nu, \vartheta, \kappa). \quad (23)$$

By applying the Karush-Kuhn-Tucker (K.K.T.) conditions, the allocated power values at the  $i^{th}$  time slot for the source and the relay nodes can be iteratively updated in the following. Taking the partial derivative of (22) with respect to  $\bar{P}_{s,i}$  and equating the result to zero, we can get a quadratic equation in terms of  $e^{\bar{P}_{s,i}}$ :

$$\omega_{s,i} \sigma_d^2 g_{sr,i} \left( e^{\bar{P}_{s,i}} \right)^2 + \omega_{s,i} \left( e^{\bar{P}_{r,i}} g_{rd,i} \sigma_r^2 + \sigma_r^2 \sigma_d^2 \right) e^{\bar{P}_{s,i}} - \left( e^{\bar{P}_{r,i}} g_{rd,i} \sigma_r^2 + \sigma_r^2 \sigma_d^2 \right) = 0, \quad (24)$$

where we define  $\omega_{s,i} = \frac{2 \log 2}{\rho_i} \left( \sum_{k=i}^T \lambda_k + \sum_{k=1}^{T-1} \vartheta_k \right)$ . From Theorem 2 and the complementary slackness condition for the constraint (C.1) in the problem (P4), it is obtained that  $\lambda_T$  is always positive, resulting in a positive summation term of  $\sum_{k=i}^T \lambda_k + \sum_{k=1}^{T-1} \vartheta_k$ . Moreover, since  $\rho_i > 0$  as defined in (15), it implies that  $\omega_{s,i} > 0$ . By applying a standard root finding formula to (24), the allocated power at the  $(t+1)^{th}$  iteration for the source node at the  $i^{th}$  time slot can be derived as in (25) shown in next page, where  $\Gamma_{rd,i}^{(t)} = e^{\bar{P}_{r,i}^{(t)}} g_{rd,i} / \sigma_d^2$  is the SNR for the second hop,  $\Psi_{sr,i} = g_{sr,i} / \sigma_r^2$  is the ratio of the channel power to the relay noise power for the first hop, and  $[x]^+ = \max(0, x)$ , which implicitly shows that the allocated power must be non-negative. Likewise, the allocated power at the  $(t+1)^{th}$  iteration for the relay node

$$\begin{aligned}
\mathcal{L}(\bar{\mathbf{P}}_s, \bar{\mathbf{P}}_r, \delta, \lambda, \mu, \eta, \nu, \vartheta, \kappa) &= \frac{1}{2} \sum_{i=1}^T \left[ \frac{\rho_i}{\log 2} \left\{ \bar{P}_{s,i} + \bar{P}_{r,i} + \log(g_{rd,i} g_{sr,i}) - \log \left( e^{\bar{P}_{s,i}} g_{rd,i} \sigma_r^2 + \sigma_d^2 \left( e^{\bar{P}_{s,i}} g_{sr,i} + \sigma_r^2 \right) \right) \right\} + \beta_i \right] \\
&\quad - \sum_{k=1}^T \lambda_k \left( \sum_{i=1}^k e^{\bar{P}_{s,i}} - \sum_{i=1}^k (E_{s,i} - \delta_i) \right) - \sum_{k=1}^T \mu_k \left( \sum_{i=1}^k e^{\bar{P}_{r,i}} - \sum_{i=1}^k (E_{r,i} + \alpha \bar{g}_{sr,i} \delta_i) \right) \\
&\quad - \sum_{k=1}^{T-1} \eta_k \left( \sum_{i=1}^{k+1} (E_{s,i} - \delta_i) - \Omega_{s,k} - E_{s,max} \right) - \sum_{k=1}^{T-1} \nu_k \left( \sum_{i=1}^{k+1} (E_{r,i} + \alpha \bar{g}_{sr,i} \delta_i) - \Omega_{r,k} - E_{r,max} \right) \\
&\quad - \sum_{k=1}^{T-1} \vartheta_k \left( \sum_{i=1}^k e^{\bar{P}_{s,i}} - \Omega_{s,k} \right) - \sum_{k=1}^{T-1} \kappa_k \left( \sum_{i=1}^k e^{\bar{P}_{r,i}} - \Omega_{r,k} \right), \tag{22}
\end{aligned}$$

$$\begin{aligned}
e^{\bar{P}_{s,i}^{(t+1)}} &= \left[ \frac{-\omega_{s,i}^{(t)} (\Gamma_{rd,i}^{(t)} + 1) + \sqrt{\omega_{s,i}^{(t)2} (\Gamma_{rd,i}^{(t)} + 1)^2 + 4\Psi_{sr,i} \omega_{s,i}^{(t)} (\Gamma_{rd,i}^{(t)} + 1)}}{2\Psi_{sr,i} \omega_{s,i}^{(t)}} \right]^+ \\
&= \left[ \frac{-(\Gamma_{rd,i}^{(t)} + 1)}{2\Psi_{sr,i}} + \frac{\sqrt{(\Gamma_{rd,i}^{(t)} + 1)^2 + \frac{4\Psi_{sr,i}}{\omega_{s,i}^{(t)}} (\Gamma_{rd,i}^{(t)} + 1)}}{2\Psi_{sr,i}} \right]^+, \quad i = 1, \dots, T, \tag{25}
\end{aligned}$$

at the  $i^{th}$  time slot is given in (26) as shown on the top of next page, where  $\Gamma_{sr,i}^{(t)} = e^{\bar{P}_{s,i}^{(t)}} g_{sr,i} / \sigma_r^2$  is the SNR for the first hop,  $\Psi_{rd,i} = g_{rd,i} / \sigma_d^2$  is the ratio of the channel power to the destination noise power for the second hop, and  $\omega_{r,i}^{(t)} = \frac{2\log 2}{\rho_i} \left( \sum_{k=i}^T \mu_k^{(t)} + \sum_{k=1}^{T-1} \kappa_k^{(t)} \right) > 0$  according to Theorem 3 and the complementary slackness condition ( $\mu_T > 0$ ) for the constraint (C.2) in the problem (P4). Moreover, by taking the partial derivative of (22) with respect to  $\delta_i$ , the power transfer value at the  $(t+1)^{th}$  iteration can be updated via a subgradient method as in (27) shown in next page, where  $\epsilon_0$  is an appropriate step size.

2) *Solution of the Master Dual Problem (Update of Lagrangian Multipliers)*: The subgradient method is utilized to find the Lagrangian multipliers  $\lambda, \mu, \eta, \nu, \vartheta$  and  $\kappa$  at the  $(t+1)^{th}$  iteration, which leads to the following updated formulas as in (28)–(33) shown in next page, where  $\epsilon_i$  is a positive step size, for  $i = 1, 2, \dots, 6$ .

With the new obtained Lagrangian multipliers, the power control and transfer values,  $\bar{P}_{s,i}^{(t+1)}$ ,  $\bar{P}_{r,i}^{(t+1)}$  and  $\delta_i^{(t+1)}$ , are updated again, and meanwhile, the lower bound performance in (13) can be further enhanced by updating the coefficients  $\rho_i$  and  $\beta_i$  using (18) [39]. Accordingly, an iterative algorithm is summarized in Table I under the fixed values of the auxiliary variables  $\Omega_s$  and  $\Omega_r$ , for which the above procedures are repeated until convergence is reached.

#### D. Convergence of the Proposed Algorithm

It is first noted that the problem (P2) is non-convex, and we resort to the introduction of auxiliary variables  $(\Omega_{s,k}, \Omega_{r,k})$  in the problem (P3) and a lower bound for the sum rate in the

TABLE I: Iterative algorithm for power control and transfer under fixed values of  $\Omega_s$  and  $\Omega_r$

- 1: Set the maximum number of iterations  $I_{max}$  and the step sizes  $\epsilon_1, \epsilon_2, \dots, \epsilon_6$ ;
- 2: Initialize the iteration counter  $t = 0$ ,  $\rho_i^{(t)} = 1$  and  $\beta_i^{(t)} = 0$ ;
- 3: Initialize  $\bar{\mathbf{P}}_s^{(t)}$ ,  $\bar{\mathbf{P}}_r^{(t)}$ ,  $\lambda^{(t)}$ ,  $\mu^{(t)}$ ,  $\eta^{(t)}$ ,  $\nu^{(t)}$ ,  $\vartheta^{(t)}$  and  $\kappa^{(t)}$ .
- 4: **repeat**
- 5:     **repeat** (Solving problem (P4))
- 6:         Update  $\bar{\mathbf{P}}_s$  and  $\bar{\mathbf{P}}_r$  using (25) and (26);
- 7:         Update  $\delta$  using (27);
- 8:         Update  $\lambda, \mu, \eta, \nu, \vartheta$  and  $\kappa$  using (28)–(33).
- 9:     **until** convergence to the optimal solution  $\bar{\mathbf{P}}_s^*$ ,  $\bar{\mathbf{P}}_r^*$  and  $\delta^*$ ;
- 10:     Update the two coefficients  $\rho_i^{(t+1)}$  and  $\beta_i^{(t+1)}$  using (15) and (16);
- 11:     Set  $\bar{\mathbf{P}}_s^{(t+1)} \leftarrow \bar{\mathbf{P}}_s^{*(t)}$ ,  $\bar{\mathbf{P}}_r^{(t+1)} \leftarrow \bar{\mathbf{P}}_r^{*(t)}$  and  $\delta^{(t+1)} \leftarrow \delta^{*(t)}$  and  $t \leftarrow t + 1$ .
- 12: **until** convergence or  $t > I_{max}$ .

problem (P4) in order to solve the problem (P2). Also note that when the auxiliary variables  $(\Omega_{s,k}, \Omega_{r,k})$  and the coefficients  $(\rho_i, \beta_i)$  are fixed, the primal problem (P4) is convex and satisfies the Slater's condition [42]. The duality gap between the primal and dual problems for (P4) is zero under the fixed auxiliary variables  $(\Omega_{s,k}, \Omega_{r,k})$  and coefficients  $(\rho_i, \beta_i)$ . In other words, the inner loop of the proposed algorithm can solve (P4) optimally under the fixed auxiliary variables  $(\Omega_{s,k}, \Omega_{r,k})$  and coefficients  $(\rho_i, \beta_i)$ .

The proposed algorithm can solve the problem (P3) optimally, while the values of the auxiliary variables  $(\Omega_{s,k}, \Omega_{r,k})$  are fixed, for  $k = 1, \dots, T-1$ . In the proposed algorithm, we solve the lower bound problem (P4) via dual decomposition for the given values of the auxiliary variables, and update the

$$\begin{aligned}
e^{\bar{P}_{r,i}^{(t+1)}} &= \left[ \frac{-\omega_{r,i}^{(t)} (\Gamma_{sr,i}^{(t)} + 1) + \sqrt{\omega_{r,i}^{(t)^2} (\Gamma_{sr,i}^{(t)} + 1)^2 + 4\Psi_{rd,i} \omega_{r,i}^{(t)} (\Gamma_{sr,i}^{(t)} + 1)}}{2\Psi_{rd,i} \omega_{r,i}^{(t)}} \right]^+ \\
&= \left[ \frac{-\left(\Gamma_{sr,i}^{(t)} + 1\right)}{2\Psi_{rd,i}} + \frac{\sqrt{\left(\Gamma_{sr,i}^{(t)} + 1\right)^2 + \frac{4\Psi_{rd,i}}{\omega_{r,i}^{(t)}} \left(\Gamma_{sr,i}^{(t)} + 1\right)}}{2\Psi_{rd,i}} \right]^+, \quad i = 1, \dots, T,
\end{aligned} \tag{26}$$

$$\delta_i^{(t+1)} = \begin{cases} \left[ \delta_i^{(t)} + \epsilon_0 \left( \sum_{k=i}^T \lambda_k - \alpha \bar{g}_{sr,i} \sum_{k=i}^T \mu_k - \sum_{k=i}^{T-1} \eta_k + \alpha \bar{g}_{sr,i} \sum_{k=i}^{T-1} \nu_k \right) \right]^+, & i = 1; \\ \left[ \delta_i^{(t)} + \epsilon_0 \left( \sum_{k=i}^T \lambda_k - \alpha \bar{g}_{sr,i} \sum_{k=i}^T \mu_k - \sum_{k=i-1}^{T-1} \eta_k + \alpha \bar{g}_{sr,i} \sum_{k=i-1}^{T-1} \nu_k \right) \right]^+, & i = 2, \dots, T, \end{cases} \tag{27}$$

$$\lambda_k^{(t+1)} = \left[ \lambda_k^{(t)} + \epsilon_1 \left( \sum_{i=1}^k e^{\bar{P}_{s,i}^{(t)}} - \sum_{i=1}^k (E_{s,i} - \delta_i^{(t)}) \right) \right]^+, \quad k = 1, \dots, T; \tag{28}$$

$$\mu_k^{(t+1)} = \left[ \mu_k^{(t)} + \epsilon_2 \left( \sum_{i=1}^k e^{\bar{P}_{r,i}^{(t)}} - \sum_{i=1}^k (E_{r,i} + \alpha \bar{g}_{sr,i} \delta_i^{(t)}) \right) \right]^+, \quad k = 1, \dots, T; \tag{29}$$

$$\eta_k^{(t+1)} = \left[ \eta_k^{(t)} + \epsilon_3 \left( \sum_{i=1}^{k+1} (E_{s,i} - \delta_i^{(t)}) - \Omega_{s,k} - E_{s,max} \right) \right]^+, \quad k = 1, \dots, T-1; \tag{30}$$

$$\nu_k^{(t+1)} = \left[ \nu_k^{(t)} + \epsilon_4 \left( \sum_{i=1}^{k+1} (E_{r,i} + \alpha \bar{g}_{sr,i} \delta_i^{(t)}) - \Omega_{r,k} - E_{r,max} \right) \right]^+, \quad k = 1, \dots, T-1; \tag{31}$$

$$\vartheta_k^{(t+1)} = \left[ \vartheta_k^{(t)} + \epsilon_5 \left( \sum_{i=1}^k e^{\bar{P}_{s,i}^{(t)}} - \Omega_{s,k} \right) \right]^+, \quad k = 1, \dots, T-1; \tag{32}$$

$$\kappa_k^{(t+1)} = \left[ \kappa_k^{(t)} + \epsilon_6 \left( \sum_{i=1}^k e^{\bar{P}_{r,i}^{(t)}} - \Omega_{r,k} \right) \right]^+, \quad k = 1, \dots, T-1, \tag{33}$$

coefficients  $\rho_i$  and  $\beta_i$  using (18) which can gradually improve the lower bound (according to Theorem 1), finally achieving the local optima of the problem (P3) with respect to the fixed auxiliary variables [39].

In fact, by fixing the auxiliary variables and following a similar proof of Theorem 1 in [39], it can be proved that when the values of the two coefficients get converged in the proposed algorithm, the corresponding optimal solution of (P4) satisfies the K.K.T. optimality conditions of the non-convex problem (P3). In other words, by fixing the values of the auxiliary variables, the obtained solution at least converges to a local maximizer for (P3) in terms of  $\bar{\mathbf{P}}_s$ ,  $\bar{\mathbf{P}}_r$  and  $\delta$ .

#### E. Finding of $\Omega_s$ and $\Omega_r$ in the Outer Loop

The remaining problem is to determine the values of the auxiliary variables  $\Omega_s$  and  $\Omega_r$  in the outer loop in order to maximize the achievable sum rate, given by

$$[\Omega_s^*, \Omega_r^*] = \arg \max_{\Omega_s, \Omega_r} \bar{f}_{LB}^*(\Omega_s, \Omega_r), \tag{34}$$

where  $\bar{f}_{LB}^*(\Omega_s, \Omega_r)$  represents the achievable sum rate obtained by the proposed algorithm in Table I with respect to  $\Omega_s$  and  $\Omega_r$ . It is impossible to exhaustively search over all values of  $\Omega_s$  and  $\Omega_r$  because the involved computational burden is high. Instead, a two-step method is proposed to determine the values of  $\Omega_s$  and  $\Omega_r$  in the outer loop. In the first step, we first relax the battery storage constraints in (13) by letting the auxiliary variables  $\Omega_{s,k}^{(0)} = \infty$  and  $\Omega_{r,k}^{(0)} = \infty$ , for  $k = 1, \dots, T-1$ , and compute the corresponding optimal power control and transfer  $(\bar{\mathbf{P}}_s^{*(0)}, \bar{\mathbf{P}}_r^{*(0)}, \delta^{*(0)})$  through the proposed algorithm in Table I. In the next step, based on the obtained solution, we then refine the optimal power control and transfer solution by updating the auxiliary variables as  $\Omega_{s,k}^{(1)} = \sum_{i=1}^k e^{\bar{P}_{s,i}^{*(0)}}$  and  $\Omega_{r,k}^{(1)} = \sum_{i=1}^k e^{\bar{P}_{r,i}^{*(0)}}$ , for  $k = 1, \dots, T-1$ . This enables us to refine the solutions of the power control and transfer by following the track of the optimal accumulated power expenditure profiles  $\Omega_{s,k}^{(1)}$  and  $\Omega_{r,k}^{(1)}$  which are obtained without concerning the battery storage constraints in the first step.

### F. Model Extension to Bi-directional Power Transfer

The proposed design framework can be extended to accommodate bi-directional (BD) power transfer as follows. The sum rate performance of the network depends on the EH profiles at the source and the relay nodes. In the uni-directional power transfer, when the source node has a worst EH profile, the sum rate performance of the network will be dominated by the first hop despite a better EH profile at the relay node. Therefore, in order to further improve the sum rate of the network, the proposed design framework can be easily extended to the scenario where power transfer is performed in a BD mode by replacing the energy causality constraints (C.1) and (C.2) and the battery storage constraints (C.3) and (C.4) in (9) as follows.

The energy causality constraints for the power control and transfer at the source and the relay nodes in time are respectively given by

$$(C.1) \quad \sum_{i=1}^k P_{s,i} \leq \sum_{i=1}^k (E_{s,i} + \bar{\alpha} \bar{g}_{rs,i} \delta_{rs,i} - \delta_{sr,i}),$$

$$k = 1, \dots, T;$$

$$(C.2) \quad \sum_{i=1}^k P_{r,i} \leq \sum_{i=1}^k (E_{r,i} + \alpha \bar{g}_{sr,i} \delta_{sr,i} - \delta_{rs,i}),$$

$$k = 1, \dots, T,$$

where  $\alpha$  and  $\bar{\alpha}$  are the power harvesting and conversion efficiency, ranging between 0 and 1, at the relay and the source nodes, respectively, and  $\bar{g}_{rs,i}$  and  $\bar{g}_{sr,i}$  indicate the channel power gains of the dedicated energy control channels from the source to the relay nodes and the reverse direction, respectively, at the  $i^{th}$  time slot. In addition,  $\delta_{sr,i}$  and  $\delta_{rs,i}$  are the amounts of transferred energy from the source to the relay nodes and the reverse direction, respectively, at the  $i^{th}$  time slot.

Moreover, the battery storage constraints stipulate that the amount of energy stored in the battery never exceeds the maximum battery capacity at the source and the relay nodes:

$$(C.3) \quad \sum_{i=1}^{k+1} (E_{s,i} + \bar{\alpha} \bar{g}_{rs,i} \delta_{rs,i} - \delta_{sr,i}) - \sum_{i=1}^k P_{s,i} \leq E_{s,max},$$

$$k = 1, \dots, T-1;$$

$$(C.4) \quad \sum_{i=1}^{k+1} (E_{r,i} + \alpha \bar{g}_{sr,i} \delta_{sr,i} - \delta_{rs,i}) - \sum_{i=1}^k P_{r,i} \leq E_{r,max},$$

$$k = 1, \dots, T-1.$$

The new sum rate maximization problem can be formulated and solved in a similar way as in the uni-direction power transfer.

## IV. SPECIAL SCENARIOS WITH INFINITE BATTERY CAPACITY AT NODES

In this section, we investigate the effect of the battery capacity at nodes on the optimal power control solution if the battery capacity goes to infinity. Capacitors are commonly exploited for a small amount of energy storage. However,

by using super capacitors as storage devices, the assumption on the infinite battery capacity in EH relay networks, where the harvested energy in the batteries at nodes has a negligible overflow probability, becomes generally true [43]. We study the special scenarios with infinite battery capacity at either the EH source node or the EH relay node. In what follows, the optimal solutions are analyzed under these two special scenarios: i)  $E_{s,max} = \infty$ , and (ii)  $E_{r,max} = \infty$ . To examine the impact of the infinite battery capacity on the optimal power control, the relay's and the source's transmit power values are predetermined in the first and the second scenarios, respectively. Before starting the analysis, the following lemma is first introduced.

**Lemma 3:** The function  $\varphi(x_i; a) = \frac{-x_i + \sqrt{x_i^2 + ax_i}}{x_i}$  is a non-decreasing function with respect to the index  $i$ , if  $x_i \geq 0$  is a non-increasing sequence with the index  $i$  and  $a \geq 0$ .

*Proof:* The function  $\varphi(x_i; a)$  can be rewritten as

$$\varphi(x_i; a) = -1 + \sqrt{1 + \frac{a}{x_i}}. \quad (35)$$

Then, it is straightforward to verify that the function  $\varphi(x_i; a)$  is non-decreasing with the index  $i$ , since  $x_i$  is non-increasing with the index  $i$  and  $a \geq 0$ . ■

### A. Infinite Source Battery Capacity ( $E_{s,max} = \infty$ )

In this scenario, the battery capacity of the source node is assumed to be unlimited, enabling all the harvested energy being completely stored into the battery. Since  $E_{s,max} = \infty$ , the battery storage constraint for the source node (C.3) in (9) is always satisfied. Hence, the corresponding optimization problem (P1) degenerates to

$$(P5) : \max_{\mathbf{P}_s \geq 0, \mathbf{P}_r \geq 0, \delta \geq 0} f_R(\mathbf{P}_s, \mathbf{P}_r)$$

$$\text{s.t. } (C.1), (C.2) \text{ \& } (C.4) \text{ in (9)}. \quad (36)$$

As a result, the optimization problem in (P4) can be rewritten as

$$(P6) : \max_{\bar{\mathbf{P}}_s, \bar{\mathbf{P}}_r, \Omega_r, \delta \geq 0} \bar{f}_{LB}(\bar{\mathbf{P}}_s, \bar{\mathbf{P}}_r)$$

$$\text{s.t. } (C.1), (C.2), (C.4) \text{ \& } (C.6) \text{ in (12)}. \quad (37)$$

Similarly, when the auxiliary variable  $\Omega_r$  is fixed, the problem (P6) is convex in terms of  $\bar{\mathbf{P}}_s$ ,  $\bar{\mathbf{P}}_r$  and  $\delta$ . By solving the corresponding dual problem as in (21)–(25), the optimal solution of  $P_{s,i}^*$  can be obtained through an iterative update:

$$e^{\bar{P}_{s,i}^{*(t+1)}} = \left( \Gamma_{rd,i}^{(t)} + 1 \right) \frac{1}{2\Psi_{sr,i}} \varphi \left( \bar{\omega}_{s,i}^{(t)} \left( \Gamma_{rd,i}^{(t)} + 1 \right); 4\Psi_{sr,i} \right),$$

$$i = 1, \dots, T, \quad (38)$$

where  $\bar{\omega}_{s,i}^{(t)} = \frac{2\log 2}{\rho_i} \sum_{k=i}^T \lambda_k^{(t)}$ , and  $t$  is an iteration index. We then examine the optimal transmission policy of the source node if the relay's power control is preset to a constant value over the time duration  $T$ , i.e., only  $P_{s,i}$  and  $\delta_i$  are considered as the optimization variables in (36) and (37). The following theorem is given.

**Theorem 4:** If the relay's transmit power  $P_{r,i}$  is constant and the channels  $g_{sr,i}$  and  $g_{rd,i}$  are both quasi-static, for  $i = 1, \dots, T$ , the optimal power control value  $P_{s,i}^*$  under  $E_{s,max} = \infty$  is non-decreasing with respect to the time index  $i$ , i.e.,  $P_{s,i+1}^* \geq P_{s,i}^*$ , for  $i = 1, \dots, T-1$ .

*Proof:* At the  $t^{th}$  iteration, it is found from (38) that  $\bar{\omega}_{s,i}^{(t)}$  is a non-increasing function with respect to the time index  $i$  because  $\lambda_k^{(t)} \geq 0$ . Moreover, since the relay's transmit power is constant and the channels are quasi-static, by the definition in (25), this implies that  $\Gamma_{rd,i}^{(t)}$  and  $\Psi_{sr,i}$  are non-negative constant values over the time duration  $T$ . By applying Lemma 3, it then concludes that  $P_{s,i}^{*(t+1)} = e^{\bar{P}_{s,i}^{*(t+1)}}$  is non-decreasing with the time index  $i$  for any iteration number  $t$ . Hence, we get  $P_{s,i+1}^* \geq P_{s,i}^*$ , for  $i = 1, \dots, T-1$ , when the iterative algorithm is converged. ■

#### B. Infinite Relay Battery Capacity ( $E_{r,max} = \infty$ )

When  $E_{r,max} = \infty$ , the relay node has infinite battery capacity for storing the harvested energy from the surrounding environment and the source node, and the battery storage constraint for the relay node (C.4) in (9) is always satisfied. For this special scenario, the optimization problem (P1) can be rewritten as

$$\begin{aligned} (\text{P7}) : \quad & \max_{\mathbf{P}_s \geq 0, \mathbf{P}_r \geq 0, \delta \geq 0} f_R(\mathbf{P}_s, \mathbf{P}_r) \\ \text{s.t.} \quad & (C.1), (C.2) \text{ \& } (C.3) \text{ in (9)}. \end{aligned} \quad (39)$$

Consequently, the optimization problem in (P4) degenerates to

$$\begin{aligned} (\text{P8}) : \quad & \max_{\bar{\mathbf{P}}_s, \bar{\mathbf{P}}_r, \bar{\Omega}_r, \bar{\delta} \geq 0} \bar{f}_{LB}(\bar{\mathbf{P}}_s, \bar{\mathbf{P}}_r) \\ \text{s.t.} \quad & (C.1), (C.2), (C.3) \text{ \& } (C.5) \text{ in (12)}. \end{aligned} \quad (40)$$

After some manipulation, which is similar to the derivation in (21)–(24) and (26), the optimal solution of  $P_{r,i}^*$  can be obtained by solving the corresponding dual problem and iteratively updated as

$$e^{\bar{P}_{r,i}^{*(t+1)}} = \left( \Gamma_{sr,i}^{(t)} + 1 \right) \frac{1}{2\Psi_{rd,i}^{(t)}} \varphi \left( \bar{\omega}_{r,i}^{(t)} \left( \Gamma_{sr,i}^{(t)} + 1 \right); 4\Psi_{rd,i}^{(t)} \right), \quad (41)$$

where  $\bar{\omega}_{r,i}^{(t)} = \frac{2\log 2}{\rho_i} \sum_{k=i}^T \mu_k^{(t)}$ . Here, we analyze the optimal power control solution of the relay node, given in (41), when the source's transmit power  $P_{s,i}$  over the entire time duration  $T$  is preset to a constant value. In result, only  $P_{r,i}$  and  $\delta_i$  are considered as the optimization variables in (39) and (40), and a theorem regarding the structure of the relay's transmit power profile is provided as follows.

**Theorem 5:** If the source's transmit power  $P_{s,i}$  is constant and the channels  $g_{sr,i}$  and  $g_{rd,i}$  are both quasi-static, for  $i = 1, \dots, T$ , the optimal power control value  $P_{r,i}^*$  under  $E_{r,max} = \infty$  is non-decreasing with respect to the time index  $i$ , i.e.,  $P_{r,i+1}^* \geq P_{r,i}^*$ , for  $i = 1, \dots, T-1$ .

*Proof:* From (41) and at the  $t^{th}$  iteration,  $\bar{\omega}_{r,i}^{(t)}$  is a non-increasing function with respect to the time index  $i$  because  $\mu_k^{(t)} \geq 0$ . Furthermore, since the channels are quasi-static

and the source's transmit power keeps constant over the time duration  $T$ , it is implied from the definition in (26) that  $\Gamma_{sr,i}^{(t)}$  and  $\Psi_{rd,i}$  are non-negative constant values, for  $i = 1, \dots, T$ . Using Lemma 3, we can conclude that  $P_{r,i}^{*(t+1)*} = e^{\bar{P}_{r,i}^{*(t+1)*}}$  is non-decreasing with the time index  $i$  for any iteration number  $t$ . Hence, we obtain  $P_{r,i+1}^* \geq P_{r,i}^*$ , for  $i = 1, \dots, T-1$ , when the iterative algorithm gets converged. ■

#### V. ALTERNATING OPTIMIZATION PROBLEM: WEIGHTED SUM-MSE MINIMIZATION

The design problem in Section II can be formulated as an equivalent weighted sum-MSE minimization problem and solved by alternating optimization. Based on the idea in [44], we can easily transform the sum rate maximization problem into a weighted sum-MSE minimization problem for the proposed design framework as follows:

Using (4), the MSE for the relay network at the  $i^{th}$  time slot is formulated as

$$\begin{aligned} Q_i &= \mathbb{E} \left\{ (\tilde{y}_{d,i} - x_{s,i}) (\tilde{y}_{d,i} - x_{s,i})^H \right\} \\ &= \mathbb{E} \left\{ (u_i y_{d,i} - x_{s,i}) (u_i y_{d,i} - x_{s,i})^H \right\} \\ &= \mathbb{E} \left\{ u_i y_{d,i} y_{d,i}^H u_i^H - u_i y_{d,i} x_{s,i}^H - x_{s,i} y_{d,i}^H u_i^H + x_{s,i} x_{s,i}^H \right\}, \end{aligned} \quad (42)$$

where  $u_i$  is an adjustable gain for the received signal  $y_{d,i}$ .

$$\begin{aligned} & \mathbb{E} \left\{ u_i y_{d,i} y_{d,i}^H u_i^H \right\} \\ &= \mathbb{E} \left\{ u_i \left\{ \frac{P_{s,i} P_{r,i}}{P_{s,i} g_{sr,i} + \sigma_r^2} h_{rd,i} h_{sr,i} x_{s,i} (h_{rd,i} h_{sr,i} x_{s,i})^H \right. \right. \\ & \quad \left. \left. + \frac{P_{r,i}}{P_{s,i} g_{sr,i} + \sigma_r^2} h_{rd,i} n_{r,i} (h_{rd,i} n_{r,i})^H + n_{d,i} n_{d,i}^H \right\} u_i^H \right\}; \\ & \mathbb{E} \left\{ u_i y_{d,i} x_{s,i}^H \right\} = \mathbb{E} \left\{ u_i \sqrt{\frac{P_{s,i} P_{r,i}}{P_{s,i} g_{sr,i} + \sigma_r^2}} h_{rd,i} h_{sr,i} x_{s,i} x_{s,i}^H \right\}. \end{aligned} \quad (43)$$

From (43) and (44),  $Q_i$  can be written as

$$\begin{aligned} Q_i &= \left| u_i \sqrt{\frac{P_{s,i} P_{r,i}}{P_{s,i} g_{sr,i} + \sigma_r^2}} h_{rd,i} h_{sr,i} - 1 \right|^2 \\ & \quad + \frac{P_{r,i} \sigma_r^2}{P_{s,i} g_{sr,i} + \sigma_r^2} |u_i|^2 g_{rd,i} + \sigma_d^2 |u_i|^2. \end{aligned} \quad (45)$$

Using (45) and energy and battery constraints (C.1) – (C.4), the weighted sum-MSE minimization problem can be formulated as [44]

$$\begin{aligned} (\text{MSE-P1}) : \quad & \min_{\substack{\{P_{s,i}\}, \{P_{r,i}\} \\ \{\delta_i\}, \{w_i\}, \{u_i\}}} \sum_{i=1}^T (w_i Q_i - \log_2 w_i) \\ \text{s.t.} \quad & (C.1), (C.2), (C.3), \text{ \& } (C.4) \text{ in (9)}. \end{aligned} \quad (46)$$

where  $w_i$  is a positive weight variable. For given  $\{P_{s,i}\}$ ,  $\{P_{r,i}\}$ , and  $\{\delta_i\}$ , the adjustable gain  $\{u_i\}$  that minimizes  $Q_i$  can be determined by taking the gradient of  $Q_i$  with respect to  $u_i^H$ ,

which is given by

$$\frac{\partial Q_i}{\partial u_i^H} = u_i \left\{ \frac{P_{s,i}P_{r,i}}{P_{s,i}g_{sr,i} + \sigma_r^2} g_{rd,i} g_{sr,i} + \frac{P_{r,i}\sigma_r^2}{P_{s,i}g_{sr,i} + \sigma_r^2} g_{rd,i} + \sigma_d^2 \right\} - \sqrt{\frac{P_{s,i}P_{r,i}}{P_{s,i}g_{sr,i} + \sigma_r^2}} h_{sr,i}^H h_{rd,i}^H. \quad (47)$$

Taking  $\frac{\partial Q_i}{\partial u_i^H} = 0$ , we get

$$u_i^* = \frac{\sqrt{\frac{P_{s,i}P_{r,i}}{P_{s,i}g_{sr,i} + \sigma_r^2}} h_{sr,i}^H h_{rd,i}^H}{\frac{P_{s,i}P_{r,i}}{P_{s,i}g_{sr,i} + \sigma_r^2} g_{rd,i} g_{sr,i} + \frac{P_{r,i}\sigma_r^2}{P_{s,i}g_{sr,i} + \sigma_r^2} g_{rd,i} + \sigma_d^2}. \quad (48)$$

The optimal weight is calculated for given  $P_{s,i}$ ,  $P_{r,i}$ ,  $\delta_i$ , and  $u_i$  as follows [29]:

$$w_i^* = Q_i^{-1}, \quad i = 1, \dots, T. \quad (49)$$

Note that the optimization problem (MSE-P1) in (46) is non-convex due to the presence of the variables  $P_{s,i}$  and  $P_{r,i}$  in numerator as well as in denominator of the objective function and the coupling of these variables. Therefore, instead of solving for their globally optimal solutions, we propose an iterative algorithm as a baseline method by adopting an alternating minimization approach similar to [45]. The detail of this algorithm is depicted as follows. For given  $u_i$  and  $w_i$ , we solve the optimization problem (MSE-P1) iteratively. Among the three variables  $P_{s,i}$ ,  $P_{r,i}$ , and  $\delta_i$ , we alternatively fix two variables and determine the third variable by solving a single-variable optimization problem. Then, we update the adjustable gain  $\{u_i\}$  and the weight  $\{w_i\}$  for the obtained  $(P_{s,i}, P_{r,i}, \delta_i)$  in the previous iteration according to (48) and (49), respectively. The aforementioned procedure is repeated until a convergent point is reached.

Next, we show that the weighted sum-MSE minimization problem is equivalent to the problem (P1) as follows:

**Theorem 6:** The weighted sum-MSE minimization problem (MSE-P1) is equivalent to the sum rate maximization problem (P1).

*Proof:* It can be proved by easily exploiting the method in [44]. ■

Further, we compare the complexity of the proposed algorithm (Algorithm-1), exhaustive search (ES) algorithm, and MSE-based iterative algorithm (Algorithm-2) as follows:

- **Algorithm-1:** To determine the optimal power control of (P4) for  $T + 1$  time intervals, we need to solve  $T + 1$  subproblems. The optimal power control and transfer solution  $(\mathbf{P}_s^*, \mathbf{P}_r^*, \delta^*)$  can be found searching over  $\mathbf{P}_s^*$ ,  $\mathbf{P}_r^*$  and  $\delta^*$ , assuming that each takes a discrete value [46]. This approach requires  $\mathcal{O}(Z^3 + 6)$  complexity, where  $Z$  is the number of power levels that can be taken by each of  $\mathbf{P}_s^*$ ,  $\mathbf{P}_r^*$  and  $\delta^*$ , and the value of six accounts for the additional linear constraints involved to solve the problem. The complexity of updating a dual variable is  $(2^e)$  (for example,  $e = 2$  if the ellipsoid method is used [47]). Therefore, the total complexity for updating dual

variables is  $\mathcal{O}(6 \times 2^e)$ . Assume that the performance converges in  $M$  iterations, and we also need to include a unit complexity for linear assignment involved in determining  $[\Omega_s^*, \Omega_r^*]$ . Thus the total complexity is given by  $\mathcal{O}(6M2^e(T + 1)(Z^3 + 6) + 2)$ .

- **Exhaustive Search (ES):** By exhaustively searching various possible values of the auxiliary variables  $\Omega_s = \{\Omega_{s,k}\}$  and  $\Omega_r = \{\Omega_{r,k}\}$ , for  $k = 1, \dots, T - 1$ , we can find the optimal solution. Suppose that each auxiliary variable has  $W$  quantized values and the algorithm converges in  $N$  iterations. When the number of the discrete values  $W$  increases, the complexity of the ES method increases very quickly. The total complexity is given by  $\mathcal{O}(6M2^e(T + 1)(Z^3 + 6)NW^2)$ .
- **Algorithm-2:** We first obtain the weights  $u_i^*$  and  $w_i^*$  by solving  $T + 1$  subproblems. The optimal power control and transfer solution  $(\mathbf{P}_s^*, \mathbf{P}_r^*, \delta^*)$  can be found by searching over  $\mathbf{P}_s^*$ ,  $\mathbf{P}_r^*$  and  $\delta^*$ , assuming two of the values as constant at a time and varying the third one until the convergence is reached. Thus the included complexity is  $\mathcal{O}((Z^2 + 4)^3)$ . Later, we update the dual variables with the complexity  $\mathcal{O}(4 \times 2^e)$ . Assume that the performance converges in  $M$  iterations for given weights and the weights converge in  $Y$  iterations. Then the total complexity is given by  $\mathcal{O}(4MY2^e(T + 1)(Z^2 + 4)^3)$ .

## VI. NUMERICAL RESULTS AND DISCUSSIONS

### A. Simulation Settings

In this section, we demonstrate the sum rate performance of the proposed power control and transfer algorithm and validate the theoretical findings in Section IV by computer simulation. The path loss models for the data transfer and the dedicated power transfer channels are both described as  $25.17 + 20 \times \log_{10}(d)$  dB ( $d$ : distance in kilometer) [48], [49]. The data channel bandwidth and the thermal noise power density are respectively given as 1 MHz and  $-174$  dBm/Hz. We set the power harvesting and conversion efficiency as  $\alpha = \bar{\alpha} = 0.3$ . The distance from the source node to the relay node and the distance from the relay node to the destination node are denoted as  $d_{SR}$  and  $d_{RD}$ , respectively, and we define a distance ratio  $r_d = d_{SR}/(d_{SR} + d_{RD})$ . The value of  $d_{SR}$  could vary from 1 m to 10 m [49], [50]. The battery capacity, if finite, is assumed to be  $E_{s,max} = E_{r,max} = 10$  mJ, and the time duration is given as  $T = 15$ , unless otherwise stated. The ambient energy is uniformly generated from three EH profiles with distinct intensity:  $E_L \triangleq [1, 15]$  mJ,  $E_M \triangleq [1, 30]$  mJ, and  $E_H \triangleq [1, 100]$  mJ, which represent the poor, medium and good EH conditions, respectively. Let  $E_s$  and  $E_r$  be the EH profiles for the source and the relay nodes, and we consider three scenarios to examine the impact of the EH capability at nodes on the sum rate performance:

- **Scenario 1** ( $E_s = E_L, E_r = E_M$  or  $E_H$ ):

In this scenario, we assume that the surrounding EH condition of the source node is poor, and the EH profile of the relay node appears to be better than that of the source node.

- **Scenario 2** ( $E_s = E_r = E_L$  or  $E_s = E_r = E_H$ ):

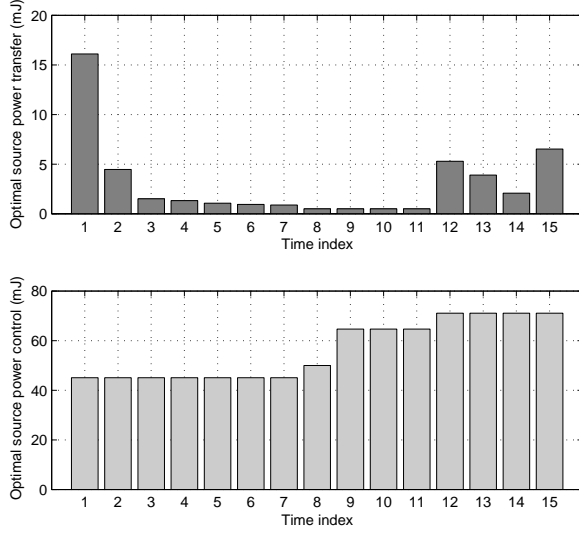


Fig. 3: An example of the optimal source power control and transfer with a preset power control value of the relay node  $P_{r,i} = 12$  mJ under  $E_{s,max} = \infty$  ( $E_s = E_H$ ,  $E_r = E_L$ ,  $d_{SR} = 1$  m, and  $d_{RD} = 50$  m).

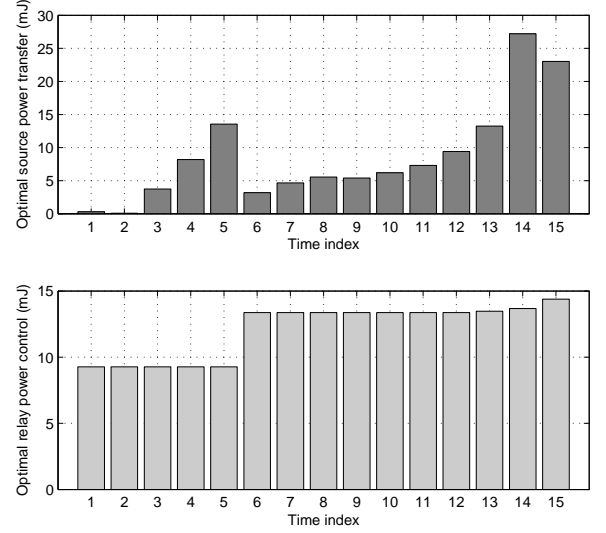


Fig. 4: An example of the optimal relay power control and source power transfer with a preset power control value of the source node  $P_{s,i} = 4.5$  mJ under  $E_{r,max} = \infty$  ( $E_s = E_r = E_M$ ,  $d_{SR} = 1$  m, and  $d_{RD} = 50$  m).

The EH conditions for both the source and the relay nodes are comparable, and thus, both nodes are assumed to have the identical EH profiles of  $E_L$  or  $E_H$ .

- *Scenario 3* ( $E_r = E_L$ ,  $E_s = E_M$  or  $E_H$ ):

The relay node suffers from a poor EH condition, whereas the source node is operated in better EH conditions with the profiles of  $E_M$  or  $E_H$ .

For the proposed algorithm, the maximum number of iterations  $I_{max}$ , the step size  $\epsilon_i$ , and the convergence tolerance are set to ten, 0.01 and  $10^{-5}$ , respectively. Finally, the average sum rate performance of the considered EH AF relay network without considering the power transfer (by setting  $\delta_i = 0$  in the considered optimization problem) and that of the direct transmission without relaying are also included for performance comparisons. Besides, we also simulate an ES method, which is used to find the globally optimal solution by searching over all variables, and the method in [25] which does not apply power transfer. In [25], a high-SNR approximation (HSA) method was adopted to tackle the non-convexity of the objective function. The battery storage constraint is applied for [25] in the simulation in order to make a fair performance comparison.

### B. Simulation Results

Two examples of the optimal power control and transfer for the source and the relay nodes in quasi-static channels  $g_{sr,i}$  and  $g_{rd,i}$  under the cases i) infinite source battery capacity,  $E_{s,max} = \infty$ , and ii) infinite relay battery capacity,  $E_{r,max} = \infty$ , are illustrated in Fig. 3 and Fig. 4, respectively. In these two figures, we set  $E_s = E_H$  and  $E_r = E_L$  for  $E_{s,max} = \infty$ , while setting  $E_s = E_r = E_M$  for  $E_{r,max} = \infty$  with  $d_{SR} = 1$  m and  $d_{RD} = 50$  m. In Fig. 3, where the power control value of the relay node is preset to  $P_{r,i} = 12$  mJ, for  $i = 1, \dots, T$ , it can be observed that the optimal power control value for the source node is non-decreasing with the

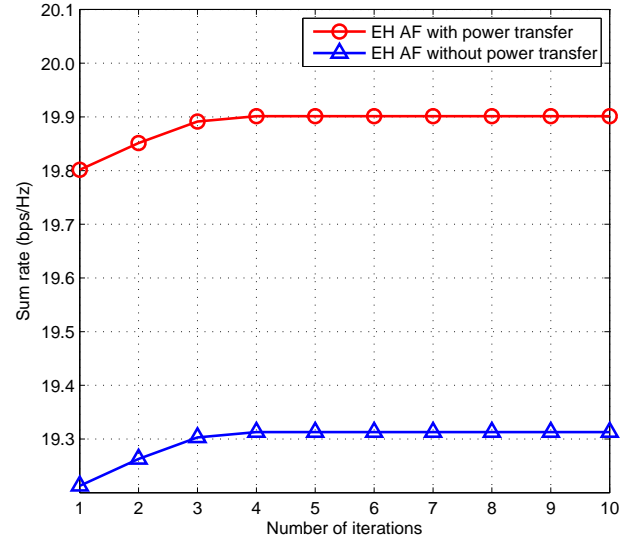


Fig. 5: Convergence behavior of the proposed algorithm ( $E_s = E_r = E_L$ ,  $d_{SR} = 1$  m, and  $d_{RD} = 50$  m).

time index  $i$ , i.e.,  $P_{s,i+1}^* \geq P_{s,i}^*$ , which confirms Theorem 4 in Section IV. Similarly, Fig. 4 validates Theorem 5 under a preset power control value of the source node  $P_{s,i} = 4.5$  mJ, and it is shown that the optimal power control value of the relay node is non-decreasing with the time index.

With a single channel realization, Fig. 5 shows the convergence behavior of the proposed algorithm in terms of the achievable sum rate under the same EH condition of  $E_L$  at both the source and the relay nodes, i.e.,  $E_s = E_r = E_L$ , where the distance values are set as  $d_{SR} = 1$  m and  $d_{RD} = 50$  m. It is observed that the sum rate is monotonically increased with the number of iterations, and the proposed algorithm requires an iteration number less than five for attaining a converged performance.

Fig. 6, Fig. 7 and Fig. 8 demonstrate the average sum

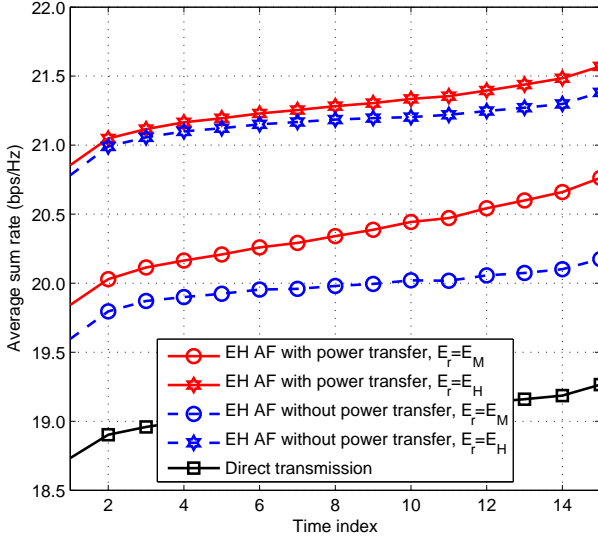


Fig. 6: Average sum rate performance versus time index in Scenario 1 ( $E_s = E_L$ ,  $d_{SR} = 1$  m, and  $d_{RD} = 50$  m).

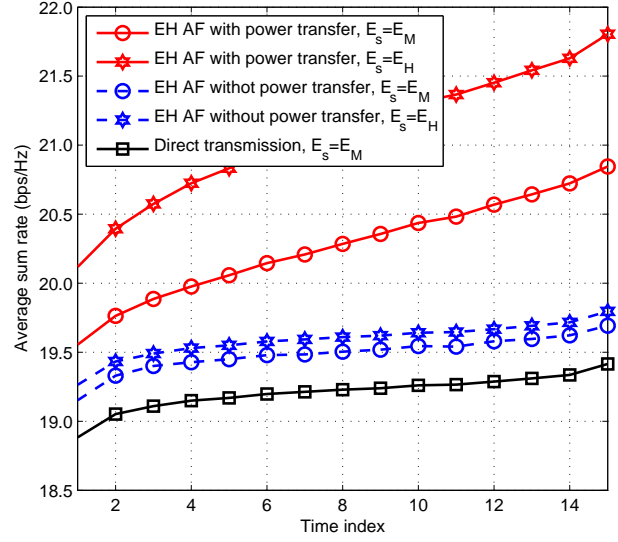


Fig. 8: Average sum rate performance versus time index in Scenario 3 ( $E_r = E_L$ ,  $d_{SR} = 1$  m, and  $d_{RD} = 50$  m).

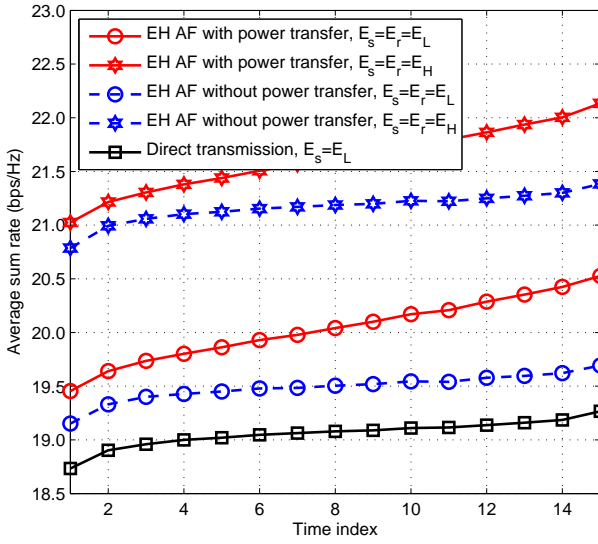


Fig. 7: Average sum rate performance versus time index in Scenario 2 ( $d_{SR} = 1$  m, and  $d_{RD} = 50$  m).

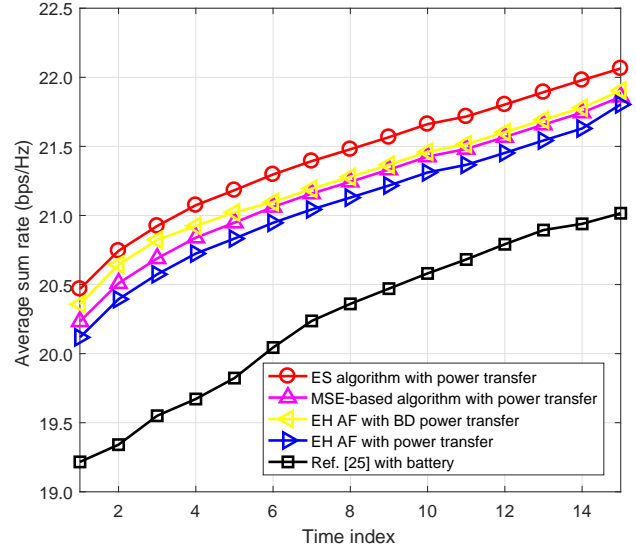


Fig. 9: Average sum rate performance for various algorithms ( $E_s = E_H$ ,  $E_r = E_L$ ,  $d_{SR} = 1$  m, and  $d_{RD} = 50$  m).

rate performance of the proposed algorithm at each time slot in Scenario 1, Scenario 2, and Scenario 3, respectively. The distance values of  $d_{SR}$  and  $d_{RD}$  are set as 1 m and 50 m, respectively. For all scenarios, it can be observed that the average sum rate with the power transfer is much superior to that without the power transfer and that only relying on the direct transmission. As observed from Fig. 6, in which the EH condition for the source node is poorer than the condition at the relay node, the average sum rate without the power transfer is closer to that with the power transfer at the beginning time slot, but the performance gap becomes wider at the end of data transmissions. A similar performance trend can be observed for the other two scenarios in Fig. 7 and Fig. 8. Interestingly, as compared with Fig. 6, one can find from Fig. 7 and Fig. 8 that the average sum rate can be significantly improved when

the source node has a better EH condition than the relay node.

Fig. 9 illustrates the sum rate performance of various algorithms. An ES method, which gives the globally optimal solution by exhaustive search, outperforms the other algorithms. The performance gap between the proposed EH AF with power transfer and the MSE-based algorithm with power transfer is quite small, and these two methods significantly outperform Ref. [25] with battery. Furthermore, due to better power utilization by both transmit nodes, the performance of the proposed algorithm with the BD power transfer is better than that with the uni-directional power transfer. In Fig. 10, we demonstrate the convergence time for the proposed algorithm and the MSE-based algorithm, and it is observed that the proposed algorithm converges faster than the MSE-based algorithm.

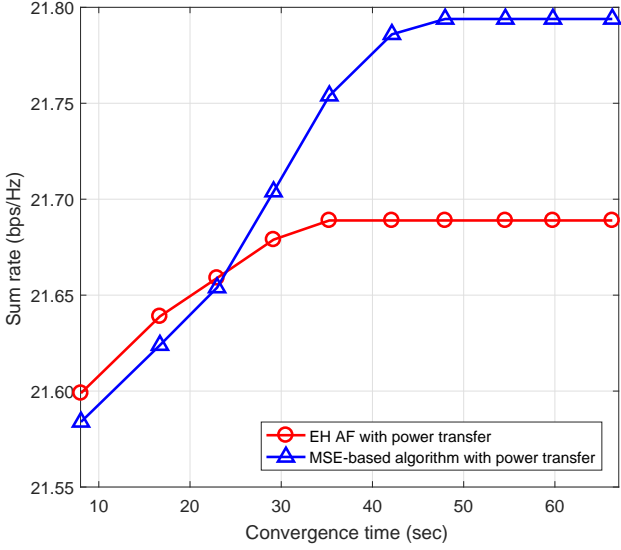
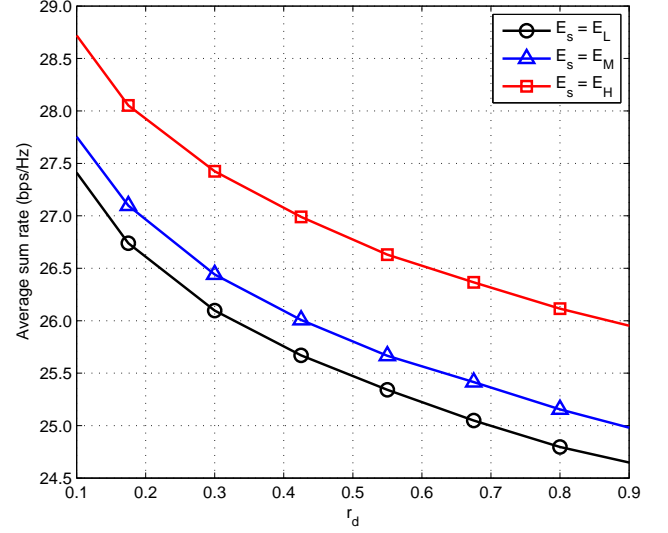


Fig. 10: Convergence time versus sum rate ( $E_s = E_r = E_H$ ,  $d_{SR} = 1$  m, and  $d_{RD} = 50$  m).

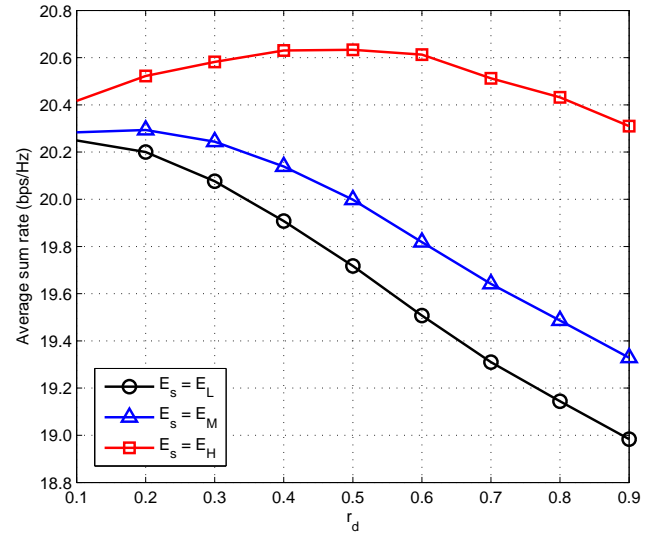
The effect of the relay's position on the average sum rate performance is shown in Fig. 11, where the total distance from the source node to the destination node,  $d_{SR} + d_{RD}$ , could be 2 m or 100 m, and  $E_r = E_H$ . It is shown from Fig. 11(a) that the highest average sum rate can be achieved when the relay node is placed in close proximity to the source node, since the amount of the harvested power transferred from the source node to the relay node is significant only for a short distance. However, for a long distance of  $d_{SR} + d_{RD} = 100$  m in Fig. 11(b), when the source node has a good EH profile, the highest average sum rate is attained when the relay node is deployed in the middle of the source and the destination nodes, while in the case of medium or poor EH profiles at the source node, the sum rate can be achieved when the relay node is located closer to the source node.

## VII. CONCLUSIONS AND FUTURE WORKS

In this paper, we investigated a joint design of power control and transfer for EH AF relay networks. The sum rate maximization problem was formulated with limited battery storage capacity and energy causality constraints at the source and the relay nodes. By applying the SCA approach and change of variables, the non-convex sum rate optimization problem was transformed into a solvable convex problem under given auxiliary variables to confine the accumulated power expenditure at nodes. Furthermore, we proposed an iterative algorithm for finding the optimal solution via dual decomposition. We showed that the performance of the EH AF relay network depends on the energy arrival profiles at the source and the relay nodes and the power transfer from the source node to the relay node. It is found that the proposed scheme outperforms the conventional direct transmission scheme without the relay. When the EH condition of the source node is poorer than that of the relay node, the performance gap between the EH relay networks with or without the power transfer is insignificant, especially when the EH condition of the relay node is also bad.



(a)  $d_{SR} + d_{RD} = 2$  m



(b)  $d_{SR} + d_{RD} = 100$  m

Fig. 11: Effect of the distance ratio on the average sum rate performance for different EH profiles with  $E_r = E_H$  (a)  $d_{SR} + d_{RD} = 2$  m and (b)  $d_{SR} + d_{RD} = 100$  m.

However, the EH relay network with a good EH condition at the source node has ability to significantly enhance the sum rate performance, as compared with the network without applying the power transfer. In addition, we studied the impact of the battery capacity and the relay position on the sum rate performance. A monotonically non-decreasing power control structure with respect to the time index was revealed for the source node and the relay node in quasi-static channels when the battery capacity at the corresponding node is infinite. Our numerical results validated the theoretical findings and quantified the impact of various factors such as EH intensity at nodes and relay position on the sum rate performance.

The theoretical findings from Theorem 2 to Theorem 5, where the accessible energy at hand should be exhausted at the end of transmissions for the source and the relay

nodes, and the power control values at nodes should be non-decreasing with the time index, can provide some guidelines for interested readers to develop online algorithms, although some ideal assumptions, e.g., infinite battery sizes and quasi-static channel gains, are made. Based on this, the power control values could be  $P_{s,i} = \min \{a_{s,i} * f_{s,i}, B_{s,i}\}$  and  $P_{r,i} = \min \{a_{r,i} * f_{r,i}, B_{r,i}\}$ , where  $f_{(\cdot),i}$  is a preset non-decreasing function,  $a_{(\cdot),i}$  is a penalty to reflect upon the instantaneous channel and battery conditions, and  $B_{(\cdot),i}$  represents the amount of energy in the batteries at time  $i$ . On the other hand, the power transfer value  $\delta_i$  could be determined by exhausting the residual energy in the battery at each time, once the power control value is decided.

For more general system models with multiple relays, power transfer between the source and the selected relays can be performed in a unidirectional/BD mode by further appending relay selection indicators to the proposed scheme. As in [28], one relay could be selected based on available battery information; however, the study of the best relay selection strategy will be a potential future direction.

## REFERENCES

- [1] Z. Hasan, H. Boostanimehr, and V. K. Bhargava, "Green cellular networks: a survey, some research issues and challenges," *IEEE J. Sel. Areas Commun.*, vol. 13, no. 4, pp. 524-540, Nov. 2011.
- [2] T. Han and N. Ansari, "On greening cellular networks via multicell cooperation," *IEEE Wireless Commun.*, vol. 20, no. 1, pp. 82-89, Feb. 2013.
- [3] T. Han and N. Ansari, "On optimizing green energy utilization for cellular networks with hybrid energy supplies," *IEEE Trans. Wireless Commun.*, vol. 12, no. 8, pp. 3872-3882, Aug. 2013.
- [4] J. N. Laneman, D. N. C. Tse, and G. W. Wornell, "Cooperative diversity in wireless networks: efficient protocols and outage behavior," *IEEE Trans. Inf. Theory*, vol. 50, no. 1, pp. 3062-3080, Dec. 2004.
- [5] M.-L. Ku, W. Li, Y. Chen, and K. J. R. Liu, "On energy harvesting gain and diversity analysis in cooperative communications," *IEEE J. Sel. Areas Commun.*, vol. 33, no. 12, pp. 2641-2657, Dec. 2015.
- [6] M. Gatzianas, L. Georgiadis, and I. Tassiulas, "Control of wireless networks with rechargeable batteries," *IEEE Trans. Wireless Commun.*, vol. 9, no. 2, pp. 581-593, Feb. 2010.
- [7] S. Ulukus, A. Yener, E. Erkip, O. Simeone, M. Zorzi, P. Grover, and K. Huang, "Energy harvesting wireless communications: a review of recent advances," *IEEE J. Sel. Areas Commun.*, vol. 33, no. 3, pp. 360-381, Jan. 2015.
- [8] J. Yang and S. Ulukus, "Optimal packet scheduling in an energy harvesting communication system," *IEEE Trans. Commun.*, vol. 60, no. 1, pp. 220-230, Jan. 2012.
- [9] K. Tutuncuoglu and A. Yener, "Optimum transmission policies for battery limited energy harvesting nodes," *IEEE Trans. Wireless Commun.*, vol. 11, no. 3, pp. 1180-1189, Mar. 2012.
- [10] C. K. Ho and R. Zhang, "Optimal energy allocation for wireless communications with energy harvesting constraints," *IEEE Trans. Signal Process.*, vol. 60, no. 9, pp. 4808-4818, Sep. 2012.
- [11] O. Ozel, K. Tutuncuoglu, J. Yang, S. Ulukus, and A. Yener, "Transmission with energy harvesting nodes in fading wireless channels: optimal policies," *IEEE J. Sel. Areas Commun.*, vol. 29, no. 8, pp. 1732-1743, Sep. 2011.
- [12] O. Ozel, J. Yang, and S. Ulukus, "Optimal broadcast scheduling for an energy harvesting rechargeable transmitter with a finite capacity battery," *IEEE Wireless Commun.*, vol. 11, no. 6, pp. 2193-2203, Jun. 2012.
- [13] B. Gurakan, O. Ozel, J. Yang, and S. Ulukus, "Energy cooperation in energy harvesting communications," *IEEE Trans. Commun.*, vol. 61, no. 12, pp. 4884-4898, Nov. 2013.
- [14] Z. Ding, S. M. Perlaza, I. Esnaola, and H. V. Poor, "Power allocation in energy harvesting wireless cooperative networks," *IEEE Trans. Wireless Commun.*, vol. 13, no. 2, pp. 846-860, Jan. 2014.
- [15] Z. Ding, S. M. Perlaza, I. Esnaola, and H. V. Poor, "Power allocation strategies in energy harvesting wireless cooperative networks," *IEEE Trans. Wireless Commun.*, vol. 13, no. 2, pp. 3543-3553, Feb. 2014.
- [16] B. Medepally and N. B. Mehta, "Voluntary energy harvesting relays and selection in cooperative wireless networks," *IEEE Trans. Wireless Commun.*, vol. 9, no. 11, pp. 846-860, Nov. 2010.
- [17] V. Raghunathan, S. Ganeriwal, and M. Srivastava, "Emerging techniques for long lived wireless sensor networks," *IEEE Commun. Mag.*, vol. 44, no. 4, pp. 108-114, Apr. 2006.
- [18] K. Huang and V. K. N. Lau, "Enabling wireless power transfer in cellular networks: architecture, modeling and deployment," *IEEE Trans. Wireless Commun.*, vol. 13, no. 2, pp. 902-912, Jan. 2014.
- [19] X. Zhou, R. Zhang, and C. K. Ho, "Wireless information and power transfer: architecture design and rate-energy tradeoff," *IEEE Trans. Wireless Commun.*, vol. 61, no. 11, pp. 4754-4767, Nov. 2013.
- [20] L. R. Varshney, "Transporting information and energy simultaneously," in *Proc. IEEE ISIT*, 2008, pp. 1612-1616.
- [21] P. Grover and A. Sahai, "Shannon meets Tesla: wireless information and power transfer," in *Proc. IEEE ISIT*, 2010, pp. 2363-2367.
- [22] R. Zhang and C. K. Ho, "MIMO broadcasting for simultaneous wireless information and power transfer," *IEEE Trans. Wireless Commun.*, vol. 12, no. 5, pp. 1989-2001, May 2013.
- [23] L. Liu, R. Zhang, and K.-C. Chua, "Wireless information and power transfer: a dynamic power splitting approach," *IEEE Trans. Commun.*, vol. 61, no. 9, pp. 3990-4001, Sep. 2013.
- [24] K. Tutuncuoglu and A. Yener, "Cooperative energy harvesting communications with relaying and energy sharing," in *Proc. IEEE ITW*, 2013, pp. 1-5.
- [25] A. Minasian, R. Adve, and S. ShahbazPanahi, "Optimal resource allocation in energy harvesting amplify-and-forward relay networks," in *Proc. IEEE GlobalSIP*, 2013, pp. 363-366.
- [26] T. P. Do, I. Song, and Y. H. Kim, "Simultaneous wireless transfer of power and information in a decode-and-forward two-way relaying network," *IEEE Trans. Wireless Commun.*, vol. 16, no. 3, pp. 1579-1592, Mar. 2017.
- [27] I. Krikidis, "Relay selection in wireless powered cooperative networks with energy storage," *IEEE J. Sel. Areas Commun.*, vol. 33, no. 12, pp. 2596-2610, Dec. 2015.
- [28] K. H. Liu, "Performance analysis of relay selection for cooperative relays based on wireless power transfer with finite energy storage," *IEEE Trans. Veh. Technol.*, vol. 65, no. 7, pp. 5110-5121, Jul. 2016.
- [29] Y. Gu, H. Chen, Y. Li, Y. C. Liang, and B. Vucetic, "Distributed multi-relay selection in accumulate-then-forward energy harvesting relay networks," *IEEE Trans. Green Commun. Netw.*, vol. PP, no. 99, pp. 1-1, Oct. 2017.
- [30] H. Chen, Y. Li, Y. Jiang, Y. Ma, and B. Vucetic, "Distributed power splitting for SWIPT in relay interference channels using game theory," *IEEE Trans. Wireless Commun.*, vol. 14, no. 1, pp. 410-420, Jan. 2015.
- [31] V. Kuhn, C. Lahuec, F. Seguin, and C. Person, "A multi-band stacked RF energy harvester with RF-to-DC efficiency up to 84%," *IEEE Trans. Microw. Theory Techn.*, vol. 63, no. 5, pp. 1768-1778, May 2015.
- [32] V. Kuhn, F. Seguin, C. Lahuec, and C. Person, "A multi-tone RF energy harvester in body sensor area network context," *Loughborough Antennas and Propagation Conf.*, Loughborough, UK, Nov. 2013, pp. 238-241.
- [33] N. Barroca, H. M. Saraiva, and P. T. Gouveia, "Antennas and circuits for ambient RF energy harvesting in wireless body area networks," *IEEE PIMRC*, London, UK, Sep. 2013, pp. 532-537.
- [34] M. Piuela, P. D. Mitcheson, and S. Lucyszyn, "Ambient RF energy harvesting in urban and semi-urban environments," *IEEE Trans. Microw. Theory Techn.*, vol. 61, no. 7, pp. 2715-2726, Jul. 2013.
- [35] H. J. Visser, C. Reniers, A. C. F. Person, and J. A. C. Theeuwes, "Ambient RF energy scavenging: GSM and WLAN power density measurements," *European Microwave Conf.*, Amsterdam, The Netherlands, Oct. 2008, pp. 721-724.
- [36] B. Clerckx and E. Bayguzina, "Waveform design for wireless power transfer," *IEEE Trans. Signal Process.*, vol. 64, no. 23, pp. 5972-5, Dec. 2016.
- [37] A. Boaventura, D. Belo, R. Fernandes, A. Collado, A. Georgiadis, and N. B. Carvalho, "Boosting the efficiency: unconventional waveform design for efficient wireless power transfer," *IEEE Microw. Mag.*, vol. 16, no. 3, pp. 87-96, Apr. 2015.
- [38] Y. Huang and B. Clerckx, "Large-scale multi-antenna multisine wireless power transfer," *IEEE Trans. Signal Process.*, vol. 65, no. 21, pp. 5812-5827, Nov. 2017.
- [39] K. Singh and M.-L. Ku, "Toward green power allocation in relay-assisted multiuser networks: a pricing-based approach," *IEEE Trans. Wireless Commun.*, vol. 14, no. 5, pp. 2470-2486, May 2015.
- [40] S. Boyd, L. Xiao, A. Mutapcic, and J. Mattingley, "Notes on decomposition methods," Apr. 2008. [Online]. Available: [http://see.stanford.edu/materials/lsoecoe364b/08-decomposition\\_notes.pdf](http://see.stanford.edu/materials/lsoecoe364b/08-decomposition_notes.pdf).

- [41] Y. Zhao, R. Adve, and T. J. Lim, "Improving amplify-and-forward relay networks: optimal power allocation versus selection," *IEEE Trans. Wireless Commun.*, vol. 16, no. 8, pp. 3114-3123, Aug. 2007.
- [42] S. Boyd and L. Vandenberghe, "Convex optimization," *Cambridge University Press*, 2004.
- [43] A. A. Nasir, X. Zhou, S. Durrani, and R. A. Kennedy, "Wireless-powered relays in cooperative communications: time-switching relaying protocols and throughput analysis," *IEEE Trans. Commun.*, vol. 63, no. 5, pp. 1607-1622, May 2015.
- [44] Q. Shi, M. Razaviyayn, Z. Q. Luo and C. He, "An iteratively weighted MMSE approach to distributed sum-utility maximization for a MIMO interfering broadcast channel," *IEEE Trans. Signal Process.*, vol. 59, no. 9, pp. 4331-4340, Sep. 2011.
- [45] K. T. Truong, P. Sartori, and R. W. Heath, "Cooperative algorithms for MIMO amplify-and-forward relay networks," *IEEE Trans. Signal Process.*, vol. 61, no. 5, pp. 1272-1287, Mar. 2013.
- [46] C. K. Ho, R. Zhang, and Y.-C. Liang, "Two way relaying over OFDM: Optimized tone permutation and power allocation," in *Proc. IEEE ICC*, pp. 3908-3912, May 2008.
- [47] W. Yu and R. Lui, "Dual methods for nonconvex spectrum optimization of multicarrier systems," *IEEE Trans. Commun.*, vol. 54, no. 7, pp. 1310-1322, Jul. 2006.
- [48] H. J. Visser and R. J. M. Vullers, "RF energy harvesting and transport for wireless sensor network applications: principles and requirements," *Proc. IEEE*, vol. 101, no. 6, pp. 1410-1423, Jun. 2013.
- [49] S. Percy, C. Knight, F. Cooray, and K. Smart, "Supplying the power requirements to a sensor network using radio frequency power transfer," *Sensors*, vol. 12, no. 7, pp. 8571-8585, Jun. 2012.
- [50] M. Y. Naderi, K. R. Chowdhury, and S. Basagni, "Experimental study of concurrent data and wireless energy transfer for sensor networks," in *Proc. IEEE GLOBECOM*, 2014, pp. 2543-2549.



**Keshav Singh (S'12, M'16)** received the degree of Master of Technology in Computer Science from Devi Ahilya Vishwavidyalaya, Indore, India, in 2006, the M.Sc. in Information & Telecommunications Technologies from Athens Information Technology (AIT), Greece, in 2009, and the Ph.D. degree in Communication Engineering from National Central University, Taiwan, in 2015. Since 2016, he has been with Institute for Digital Communications, School of Engineering, University of Edinburgh, UK, where he is currently working as a Research

Associate. He has also served as a Technical Program Committee Member for numerous IEEE conferences. His current research interests are in the areas of Green Communications, Resource Allocation, Full-Duplex Radio, Cooperative and Energy Harvesting Networks, Multiple-Input and Multiple-Output (MIMO), Non-Orthogonal Multiple Access (NOMA), and Wireless Caching.



**Meng-Lin Ku (M'11)** received the B.S., M.S., and Ph.D. degrees from National Chiao Tung University, Hsinchu, Taiwan, in 2002, 2003, and 2009, respectively, all in communication engineering. Between 2009 and 2010, he was a Postdoctoral Research Fellow with Prof. Li-Chun Wang in the Department of Electrical and Computer Engineering, National Chiao Tung University and with Prof. Vahid Tarokh in the School of Engineering and Applied Sciences, Harvard University. In August 2010, he became a Faculty Member of the Department of Commu-

cation Engineering, National Central University, Jung-li, Taiwan, where he is currently an Associate Professor. During the summer of 2013, he was a Visiting Scholar in the Signals and Information Group of Prof. K. J. Ray Liu at the University of Maryland. Dr. Ku was a recipient of the Best Counseling Award in 2012 and the university-level Best Teaching Award in 2014, 2015 and 2016 at National Central University. He was also the recipient of the Exploration Research Award of the Pan Wen Yuan Foundation, Taiwan, in 2013. His current research interests are in the areas of green communications, cognitive radios, and optimization of radio access.



**Jia-Chin Lin (S'95-M'98-SM'03)** received a B.S. and a M.S. degree from the Department of Electronics Engineering at National Chiao Tung University (NCTU) in Taiwan in 1994 and 1995, respectively, and a Ph.D. degree from National Taiwan University (NTU) in Taiwan in 1998.

Jia-Chin Lin was in the obligatory military service from July 1998 to March 2000 and then joined the Microelectronics and Information Systems Research Center at NCTU as a Research Assistant Professor. In February 2001, he joined the Department of Electrical Engineering at National Chi Nan University (NCNU) in Taiwan as an Assistant Professor. In August 2004, he was promoted to serve as an Associate Professor. From July to August of 2004 and from August 2005 to July 2006, he held the visiting associate professorship in the Department of Electrical Engineering at Stanford University. In August 2006, he joined the faculty in the Department of Communication Engineering at National Central University (NCU) in Taiwan as an Associate Professor. In August 2008, he was promoted to serve as a Full Professor. In January 2011, he became a Distinguished Professor. He had served as the Chairman in the Department of Communication Engineering at NCU from August 2011 to July 2014. From July 2014, he has been serving as a visiting fellow in the Department of Electrical Engineering, Princeton University. His research interests include wireless transmission technologies, signal processing for communications and signal synchronization techniques.

Jia-Chin Lin has been serving as an (Associate) Editor for the IEEE Transactions on Vehicular Technology from 2008. He has been serving as a Technical Associate Editor for IEEE Communications Magazine from 2013. He had served as an Associate Editor for the IEEE Signal Processing Letters from 2011 to 2012. He served as a Guest Editor for the IEEE Journal on Selected Areas in Communications (Special Issue on Emerging Technologies in Communications: Vehicular Networks and Telematics Applications.) He served as a Guest Editor for IEEE ITS Magazine and a Guest Editor for IET ITS. He served as the Lead Guest Editor for the IEEE Transactions on Vehicular Technology (Special Issue on Telematics Advances for Vehicular Communication Networks) in 2011. He delivered a keynote speech titled Recent Advances on Signal Synchronization at the International Conference on Recent Advances in Information Technology (RAIT), March 15-18, 2012, Dhanbad, India. He also serves as a Technical Program Committee Member for numerous IEEE conferences and as a reviewer for IEEE and IET journals.

Jia-Chin Lin has published more than 30 papers in international journals, authored/co-authored 6 book chapters, presented more than 40 papers at international conferences, edited 2 books and had one patent. He had also served as the Vice Chair of Meetings and Conferences Committee for the 2008-2009 IEEE AP ComSoc. Jia-Chin Lin has won many awards, including the Dr. Wu Da-You Research Award from the National Science Council (NSC), Executive Yuan, the 2003 Award for Outstanding Faculty from the Ministry of Education, the Young Scientist Award issued by URSI, the Outstanding Researcher Award from the IEEE ComSoc APB, the Investigative Research Award (for visiting scholarship) from the Pan Wen Yuan Foundation, and the Taiwan Merit Scholarships (TMS) Program from Executive Yuan. Professor Lin also won the 2009 Ten Outstanding Young Persons Award of Taiwan. He is a Fellow of the IET and a Senior Member of IEEE.



**Tharmalingam Ratnarajah (A'96-M'05-SM'05)** is currently with the Institute for Digital Communications, University of Edinburgh, Edinburgh, UK, as a Professor in Digital Communications and Signal Processing. His research interests include signal processing and information theoretic aspects of 5G and beyond wireless networks, full-duplex radio, mmWave communications, random matrices theory, interference alignment, statistical and array signal processing and quantum information theory. He has published over 330 publications in these areas and holds four U.S. patents. He was the coordinator of the FP7 projects ADEL (3.7M€) in the area of licensed shared access for 5G wireless networks and HARP (4.6M€) in the area of highly distributed MIMO and FP7 Future and Emerging Technologies projects HIATUS (3.6M€) in the area of interference alignment and CROWN (3.4M€) in the area of cognitive radio networks. Dr. Ratnarajah is a Fellow of Higher Education Academy (FHEA), U.K..